We highly appreciated the critical but extremely constructive reviewer comments and their thoughtful suggestions. Based on these comments we carefully revised our manuscript. Below you will find our point-by-point response to the reviewer´s comments and suggestions, as well as the corresponding changes in the manuscript. The revised data set was uploaded to the repositories and is available under https://doi.org/10.5281/zenodo.3733202 and https://doi.org/10.11888/Meteoro.tpdc.270333 (Version 2).

In the name of all co-authors,

Felix Nieberding

Response to Anonymous Referee #1

Dear referee, thank you very much for your positive assessment of our manuscript. It is appreciated that the added value of our study is seen by the scientific community, especially with regard to the extensive documentation of the data set.

Response to Anonymous Referee #2

Major points:

1. **WPL and SSH correction:**

Reviewer comment 1: After WPL and SSH you still have a diurnal cycle in the CO2 data even during winter. Obviously, this pattern is not real but this is not at all discussed in the manuscript. This is most likely a WPL correction effect and not a physiological meaningful signal.

Response to reviewer comment 1: We thoroughly re-considered the SSH correction. In the process we found that the correction approach by Oechel et al. (2014) which we used before should not be applied to our data because not all requirements are fulfilled at our study site. Hence it was removed from the data set and the manuscript. The de facto standard SSH correction following Burba et al. (2008) has been used widely at cold ecosystem flux sites (e.g. Miller et al., 2011; Webb et al., 2016) but has also been modified frequently because it has been shown to produce unsatisfactory results (Kittler et al., 2017; Oechel et al., 2014). In order to overcome this problem, we now provide the following CO2 flux time series: (1) no SSH correction applied, (2) SSH correction following Burba et al. (2008) applied, and additionally, (3) SSH correction following Frank and Massman (2020) applied. The latter approach was chosen because it corrects significant errors of the method of Burba et al. (2008).

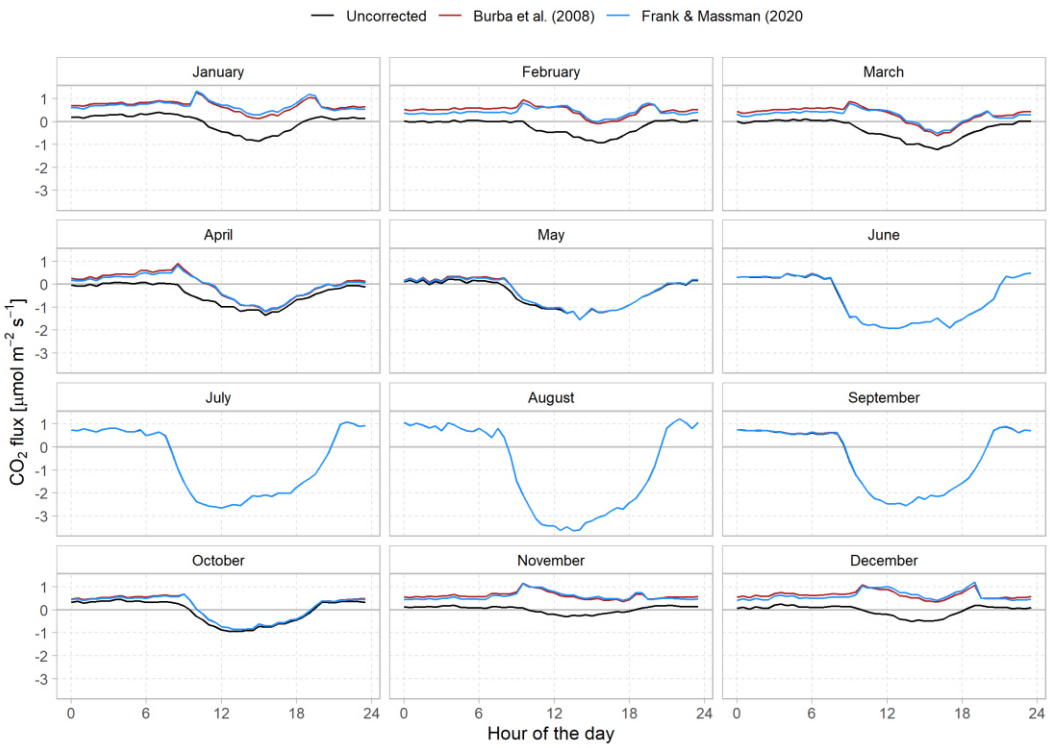

Fig. 1: The new Fig. 7 in the manuscript: Monthly mean daily course and annual course of daily mean of the CO2 flux of the years 2005 to 2019 before and after sensor self heating correction following Burba et al. (2008) and Frank and Massman (2020).

The monthly mean diurnal course of the three CO2 flux time series clearly show the effect of the SSH corrections during the cold months (Fig. 1). The effect of the two approaches of Burba et al. (2008) and Frank and Massman (2020) are very similar. We see various problems associated with the SSH corrections: (1) the corrections create strong artifacts during the transition between day and night, (2) SSH-corrected night-time CO2 fluxes during the cold months are very high – at about the same level as night-time CO2 fluxes during summer – suggesting an over-correction of SSH effects, and (3) the winter-time diurnal course of CO2 flux with day-time uptake of CO2 – which is assumed to be the effect of the SSH – does not disappear, but the daytime CO2 flux is merely offset by what seems to be a more or less constant flux value. This leads us to the conclusion that the effect of the SSH is very small at our site and that the application of the standard correction (Burba et al., 2008) and its improved version (Frank and Massman, 2020) lead to an undue over-correction of this effect. Furthermore, it leads us to the assumption that there is a real day-time CO2 uptake during winter. This could be explained by the scarce snow cover and the generally high solar radiation at our site. Measurements of surface temperature (soil temperature in 0 cm depth) show temperatures well above 0 °C during daytime in winter (mostly between 12:00 and 18:00, see Fig. 2). Plants may photosynthesize until below -3 °C, at least they do so in Antarctic tussock grass (Bate and Smith, 1983). Lichens may photosynthesize under even colder conditions (Kappen et al., 1996).

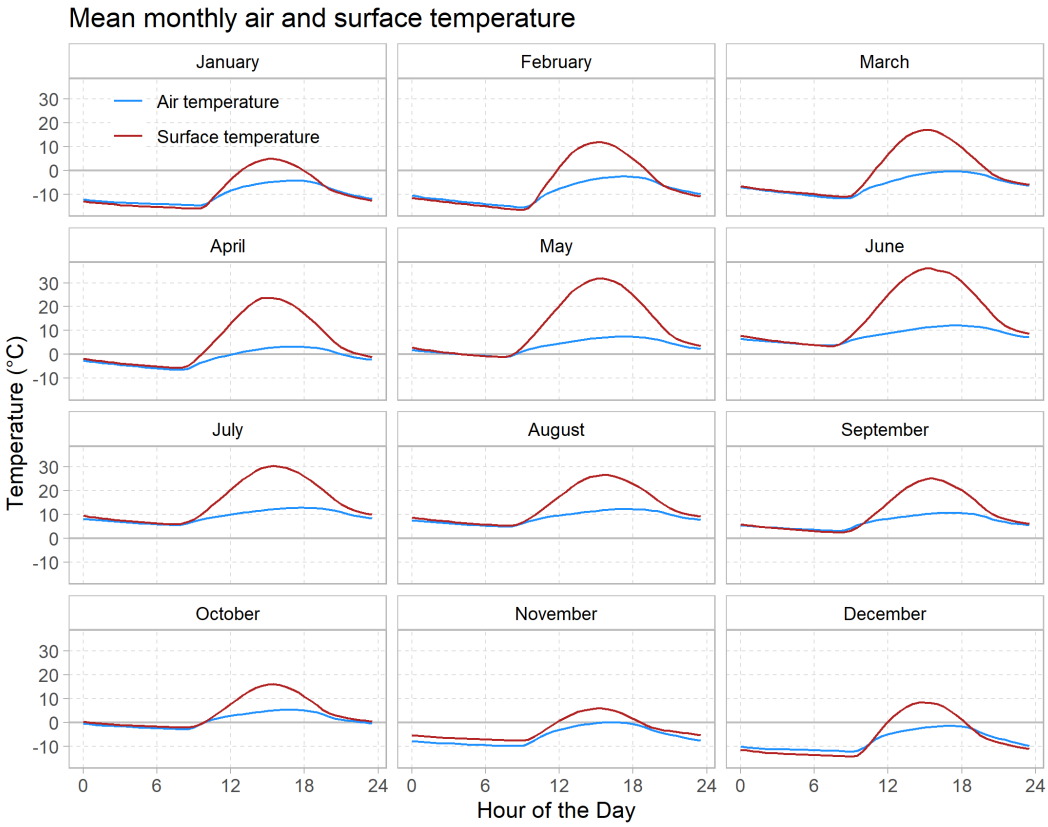

Fig. 2: Monthly mean diurnal curse of air and soil surface temperature.

To test our conclusion about the SSH effect at our site, we calculated the mean diurnal course of CO2 fluxes during cold periods with a closed snow cover (Fig. 3). Under these (rare) conditions, we expect a negligible CO2 uptake, so the SSH effect should become visible. Indeed, the not SSH-corrected CO2 flux shows only a very small diurnal pattern with CO2 uptake during daytime. This could still be a real physiological signal due to snow free patches in the EC footprint, or the SSH effect, or a combination of both. In any case, the daytime CO2 uptake under these conditions and hence the SSH effect at our site is very small. In contrast, both the SSH corrections create large positive offsets in the CO2 flux which are clearly an overcompensation of the SSH effect. In summary, we suggest that the CO2 uptake during winter represents a physiologically meaningful signal and not an artifact from incomplete SSH corrections. Nevertheless, CO2 fluxes with applied SSH correction will be part of the updated data set. A paragraph describing the issue was introduced into Sect. 2.5, 3.3 and this topic was raised in the discussion and conclusions as well.

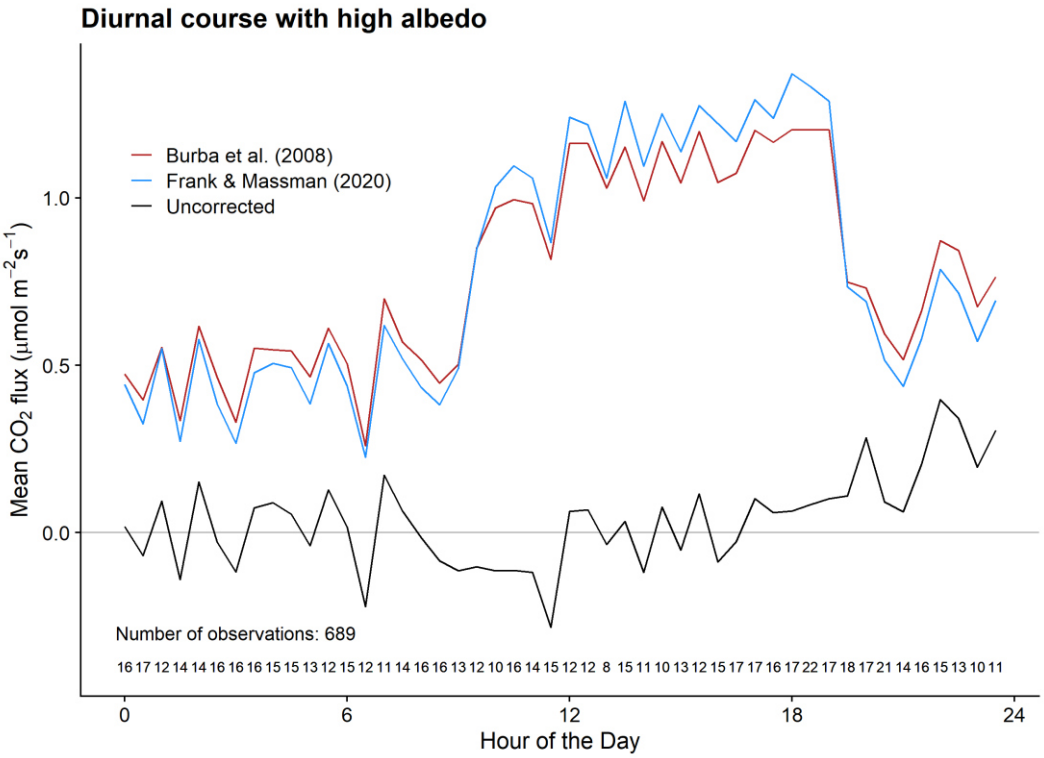

Fig. 3: Mean diurnal course of the original and SSH corrected (Burba et al., 2008; Frank and Massman, 2020) CO2 flux, during cold periods (air temperature < 0 °C) and closed snow cover (short wave albedo > 0.8). Note that a closed snow cover is rarely found at our site, therefore the number of data points is limited. Most data originate from the winter of 2006-2007.

Changes in the manuscript concerning comment 1: The SSH correction following Oechel et al. (2014) was discarded throughout the manuscript.

We added a description of the revised formulation following Frank and Massman (2020) to the Methods Sect. 2.5 *Sensor self heating correction*: “In a recent publication, Frank and Massman (2020) tested the correction procedure for a "cold, windy, high-elevation mountainous site" and found inconsistencies in the Burba et al. (2008) correction: (1) The Burba et al. (2008) correction contains boundary layer adjustment terms for non-flat surfaces but the top- and bottom surfaces of the Li-7500 are flat. This leads to an underestimation of the surface heat fluxes which is an order of magnitude too small. (2) The weightings of the bottom and top surface heat fluxes are "improbable and an order of magnitude too large" (Frank and Massman, 2020). While these errors canceled out during the study of Frank and Massman (2020), this may not be the case for other field sites. Following the recommendations of Frank and Massman (2020), we discarded the boundary layer adjustment terms for non-flat surfaces from the calculations and applied their newly calculated weightings of the bottom and top surface heat fluxes, thus emphasizing the role of the spar in self heating. We first reproduced the Burba et al. (2008) correction like it is implemented in EddyPro and then adjusted the equations as described above.”

Correspondingly, we redesigned Fig. 7 in the manuscript (Fig. 1 above) and the Results Sect. 3.3 *Sensor self heating correction* was completely reformulated: “The monthly mean diurnal course of the three CO2 flux time series in Fig. 7 clearly shows the effect of the sensor self heating correction during cold conditions (air temperature < 0 °C). The effect of the correction procedure following Burba et al. (2008) and the revised equations of Frank and Massman (2020) are very similar. We see various problems

associated with the SSH corrections: (1) the corrections create strong artifacts during the transition between day and night, (2) SSH-corrected nighttime CO2 fluxes during the cold months are very high – at about the same level as the nighttime CO2 fluxes during summer – suggesting an over-correction of SSH effects, and (3) the winter-time diurnal course of CO2 flux with daytime uptake of CO2 – which is assumed to be the effect of the SSH – does not disappear, but the daytime CO2 flux is merely offset by what seems to be a more or less constant flux value. This leads us to the conclusion that the effect of the SSH is very small at our site and that the application of the standard correction (Burba et al., 2008) and its improved version Frank and Massman (2020) lead to an undue over-correction of this effect. To test our conclusion about the SSH effect at our site, we calculated the mean diurnal course of CO2 fluxes during cold periods with a closed snow cover (Fig. A1). Under these (rare) conditions, we expect a negligible CO2 uptake, so the SSH effect should become visible. Indeed, the not SSH-corrected CO2 flux shows only a very small diurnal pattern with CO2 uptake during daytime. This could still be a real physiological signal due to snow free patches in the EC footprint, or the SSH effect, or a combination of both. In any case, the daytime CO2 uptake under these conditions and hence the SSH effect at our site is very small. In contrast, both the SSH corrections create large positive offsets in the CO2 flux which are clearly an overcompensation of the SSH effect."

And this issue was raised in the Discussion (Sect. 4): "We found the SSH effect to be rather small at our study site and moreover, the SSH corrections following Burba et al. (2008) and Frank and Massman (2020) clearly overcompensated the effects. Furthermore, we assume that there is a real daytime CO2 uptake during winter at our study site. This could be explained by the scarce snow cover and the generally high solar radiation even during the coldest months. Measurements of surface temperature (soil temperature in 0 cm depth) show temperatures well above 0 °C during daytime in winter (mostly between 12:00 and 18:00, see Fig. A2). Plants may photosynthesize until below -3 °C, at least they do so in Antarctic tussock grass (Bate and Smith, 1983) and lichens may photosynthesize under even colder conditions (Kappen et al., 1996). In summary, we suggest that the CO2 uptake during winter daytime represents a physiologically meaningful signal rather than an artifact from the SSH effect. Further research should be performed to better disentangle the two effects, hence we provide the following CO2 flux time series: (1) no SSH correction applied, (2) SSH correction following Burba et al. (2008) applied, and additionally, (3) SSH correction following Frank and Massman (2020) applied."

And in the Conclusions (Sect. 5): "Furthermore, we found that the sensor self heating effect during cold conditions only plays a minor role at our study site. When applying the standard Burba et al. (2008) self heating correction and the revised formulations by Frank and Massman (2020), we clearly see an overcompensation of the SSH effect. High solar radiation and midday soil surface temperatures well above 0 °C suggest that the small carbon uptake during winter daytime may indeed be a physiological meaningful signal rather than an artifact."

The Figs. 2 and 3 were added to the manuscript where they correspond to Figs. A1 and A2, respectively.

2. The buildings:

Reviewer comment 2: The wind disturbance due to the buildings is basically argued away even though the problem still remains. The easiest solution would be the removal of the wind direction 230 – 300 degree. Maybe account for the years and increase the angles based on the years when the respective buildings were constructed. I fully understand that you want to keep as many data as possible but the undisturbed wind field is not given at all if there are massive buildings so close to the tower. Additionally, the footprint calculation have basically no value as the assumptions of a homogeneous terrain and wind flow are strongly violated. It is a shame that the buildings were build there. The consequence is that you can't use the data and that must be faced. Further, I assume the buildings are creating heat and CO2, greenhouse maybe even contribute to a CO2 sink. All these influences can't be accounted for that is why it is required to remove these data. This simple plot gives some nice indication when things changed and how they influenced the wind field of the sonic. A slightly tilted sonic in flat terrain would have a sine shape. Here you can see the obstacles and how they influence the wind field and when things changed. This could let you also think about the size of the sectors for the planar fit methods (just as an idea). The wind coming from the back of the sonic in a set up as you have (CSAT) it should generally be removed due to flow distortion. That would be something like 350 – 10 degree.

Response to reviewer comment 2: The sine shape of the wind direction vs. unrotated vertical wind component indeed hints at a vertical tilt of the sonic anemometer that occurred during 2006 and 2007. Furthermore, the orientation of the sonic anemometer was changed from 135 degrees to 200 degrees in 2009. This was accounted for by calculating the planar fit coordinate rotation only for times when the orientation of the sonic anemometer remained constant. The dates were derived visually by analyzing the second rotation angle (pitch), estimated from a preliminary raw data processing using the double rotation method. The planar fit sectors were chosen to account for possibly disturbed turbulence from the direction of the buildings and the sensor attachment to the mast. In the paper we state that the planar fit sectors are 0° - 80°, 80° - 230 ° and 230° - 360 ° but in fact we used the following sectors: 80° - 240°, 240° - 320° and 320° - 80°. We sincerely apologize for this error and corrected it in the manuscript.

As the reviewer pointed out correctly, the assumption of a homogeneous terrain and undisturbed flow regime may not be fulfilled for all sectors. Hence, we agree that it is difficult to exclude data based on a footprint model that relies on these assumptions. We agree with the reviewer that the data from the disturbed sectors has to be excluded. We introduced an additional quality flag (qc_wind_dir), indicating whether a 30-min flux originates from a disturbed wind sector. We assume the turbulent signal to be disturbed due to (i) the back of the Csat3, (ii) the PBL container and (iii) the main buildings. The correcponding times and wind directions can be found in Tab. 1. These fluxes are excluded from subsequent analyses.

Table 1 Disturbed wind sectors

From	To	Back of USA	PBL container	Main buildings
2005-12-04	2009-06-30	305°–325°	-	260°–280°
2009-06-30	2010-01-30	10°–30 °	30°–50°	260°–280°
2010-01-30	2011-12-31	10°–30 °	30°–50°	250°–300°
2012-01-01	2018-12-31	10°–30 °	30°–50°	250°–315°

2019-01-01	2019-09-07	10°–30 °	30°–50°	245°–315°

Changes in the manuscript concerning comment 2: The footprint calculation was completely omitted throughout the manuscript.

In the Sect 2.1 *Site description and measurements* we added information about the change of the anemometer orientation and the installation of the KH50: “In June 2009, the sonic anemometer alignment was changed from 135 degrees to 200 degrees. In 2010, a KH50 krypton hygrometer was installed but the data is not available due to quality constraints.”

In the Sect. 2.2 *Raw data processing* we added information about the vertical tilt of the USA: “During 2006 and 2007 the sonic anemometer exhibited a step wise downward vertical tilt of up to 13 degrees. This was accounted for by calculating the planar fit coordinate rotation only for times when the orientation of the sonic anemometer remained constant. The dates were derived visually by analyzing the second rotation angle (pitch), estimated from a preliminary raw data processing using the double rotation method.”

The Methods Sect. 2.5 *Wind field analysis* was omitted and the information about the disturbed sectors was added to Sect. 2.4 *Quality filtering*: “During the long measuring period, spanning nearly 15 years, several buildings and scientific infrastructure were constructed in close vicinity of the eddy covariance tower. During the development of the NAMORS, from the foundation with only a few tents in 2005 to a well-equipped research station in 2019, we approximated five times with significant changes in constructions. In 2009 the PBL container, the shed and the solar panel were set up. In 2010 the main building and the green house were constructed. In 2012 the shed was rotated to become the laboratory and the tool shed next to the greenhouse was added. Finally, in 2019 the garage was relocated and extended south of the laboratory and the solar panels were removed. To assess possible influences on the flow and turbulence regime, we analyzed the wind direction distribution of the mean wind speed and the turbulent kinetic energy. We accounted for possibly disturbed turbulence, by applying the planar fit axis rotation for three different wind sectors during flux calculation (see Sect. 2.2). Furthermore, we generated a quality flag (qc_wind_dir) indicating whether a flux originates from a disturbed sector. Table 2 shows the disturbed sectors which were excluded from subsequent calculations.”

The Results Sect. 3.3 *Wind field analysis* was omitted and partially merged with Sect. 3.2 *Data availability and quality filtering.*

3. CO2 concentration correction:

Reviewer comment 3: Here a novel data correction method is introduced. The correction seems reasonable but it has not been tested, nor have uncertainties and problems been investigated? There are quite some differences between Mauna Loa and e.g. Mt. Waliguan the closest station to NAMORS I saw at https://www.esrl.noaa.gov/gmd/. What would be the differences using one or the other for the flux calculations? Of course, one can run the analysis for 50 other atmospheric CO2 background stations and see how the fluxes change but we are still missing the truth at the site. If such a method is to be used it must be thoroughly evaluated and this has not happened. Even if this correction is valid for the flux calculation it is for sure not valid to sell the resulting CO2 concentrations as the measured concentrations. If the data have not been measured by the instrument the qc-flag must be 2 and not 0. I would also like to address one point which I guess Mr. Fratini can help with or at least validate. His paper from 2014 was done with a LI7200 (and a LI7000 as reference) which is an enclosed instrument using an inlet and in best case a filter that ensures that the inside of the sensor stays clean. . As you described it you used a LI7500 open path sensor that besides the changes in the offset and the span is also highly affected by the dirt accumulating on the windows. But this effect cannot be simply calculated back, correct? If I remember correctly the LI7500 puts out the "automatic gain control" (AGC) as an indication how clean/dirty the windows are. And, there are recommendations to which AGC-value data should be used or discarded. If you have any change to get this value out of the raw data t would for sure help you to better QC the data. The CO2 concentration data in the data file are now following on average Mauna Loa but can we assume this is correct? The half hourly data show a gigantic scatter in mixing ratios between 0 and 600 ppm. Throughout the measuring period there are values of 0 in CO2 concentration. This is interesting because when using the "qc_co2_flux_composite" filter and only select data when "qc_co2_flux_composite" is equal to zero there are many of these 0-concentration data left. In fact, there are 612 data point for which CO2 concentrations are below 300 ppm (including zero-values) or above 600ppm and fluxes seem to be of high quality. This means that the fluxes have been calculated from an average concentration of 0. Does that make any sense? I would say no. You might say who cares about 612 points in a data set of 241178 but it shows that the QC scheme is still including errors. I'm honestly not convinced by this correction method especially because it was not developed for an instrument where changes in absorption might also arise from dirt on the windows. And because it was not tested and cannot be evaluated with the current data set. I'm sorry for being so negative about this correction but I hope I made my point clear and you share my point of view.

Response to reviewer comment 3: We thank the reviewer for raising these critical questions. However, we only partially agree with the reviewer´s opinion. In the following, we will address the reviewer´s comments separately and try to explain, why the correction is still valid and even more, enhances the overall accuracy (and precision) of the presented data set.

3.1 Applicability of the drift correction method

The drift correction procedure that was applied to our data set is not a novel approach. Fratini et al. (2014) introduced, described and tested the correction and it has been implemented in the Integrated Carbon Observation System (ICOS) raw data processing protocol (Sabbatini et al., 2018). It is derived analytically from the technical characteristics of the LiCor IRGAs with dual wavelength – single path design (Li-7500 and Li-7200), and it has a very clear rationale. In fact, the correction is nothing else than an analytically rigorous re-calibration of the raw data. The correction can be applied regardless of the reason for the concentration drift, be it aging of analyzer components, thermal effects, or – as

in our case – contamination of the windows in the optical path of the sensor. The concentration drift results from an absorptance offset that causes a shift of the analyzer operating point to a different region on the absorptance-concentration calibration curve. Because this calibration curve is nonlinear, a change of the operating point leads not only to the observed offset of the mean measured gas density from the real value but also to a bias in the evaluation of density fluctuations, i.e. a change of the "span calibration" (see Fig. 2 in Fratini et al., 2014). The drift correction addresses both these effects and eliminates the associated biases. In fact, the correction procedure is basically valid for any instrument with curvilinear calibration for which a reference concentration can be established.

3.2 CO2 concentration reference time series

We agree that the drift correction depends on the availability of a CO2 reference, i.e. un-biased, gas concentration time series. While this is easy to achieve for H2O, where the reference can be calculated from a meteorological air temperature and relative humidity probe, it is difficult to achieve for CO2 at our site. In our approach, we used the concentration time series from the Mauna Loa observatory because it provided the best temporal coverage and resolution for the time period of our data set. In order to generate the reference CO2 time series at 30-minute resolution we fitted the following model to the Mauna Loa concentration data

$$CO_{2\,ref} = p_1 + p_2*t + p_3*\cos(2*\pi*t/365) + p_4*\sin(2*\pi*t/365) + p_5*\cos(4*\pi*t/365) + p_6*\sin(4*\pi*t/365),$$

where t is the decimal time in days and p_i are the fit parameters. The rationale behind the use of this model rather than a linear or spline interpolation was (1) to mimic the general pattern of the atmospheric background CO2 concentration while excluding short term CO2 variations which very likely do not affect the Mauna Loa observatory and our site at the same time, and (2) to be able to better fill larger data gaps in the observatory CO2 concentration time series including the possibility to extrapolate the time series (e.g. 2019 data was not yet available at the time of data processing).

As discussed in Sect. 4 in the manuscript, there is a good agreement between the thus derived CO2 reference and the CO2 measurements at our site when the gas analyzer had been freshly calibrated (Fig. 4). At these times, the daily median of measured CO2 concentration is approximately 10-15 ppm lower than the reference. An underestimation of 15 ppm around 400 ppm means about 3.75 % error in concentration, which leads to roughly 1.5 % error in flux for CO2 (the % error in flux is roughly 40 % of the % error in concentration). Considering that the measured concentrations are often 100 to several 100 ppm away from the (assumed) real concentration and that this causes great errors in the raw flux and the WPL correction, the drift correction based on our CO2 reference can be expected to greatly reduce these errors.

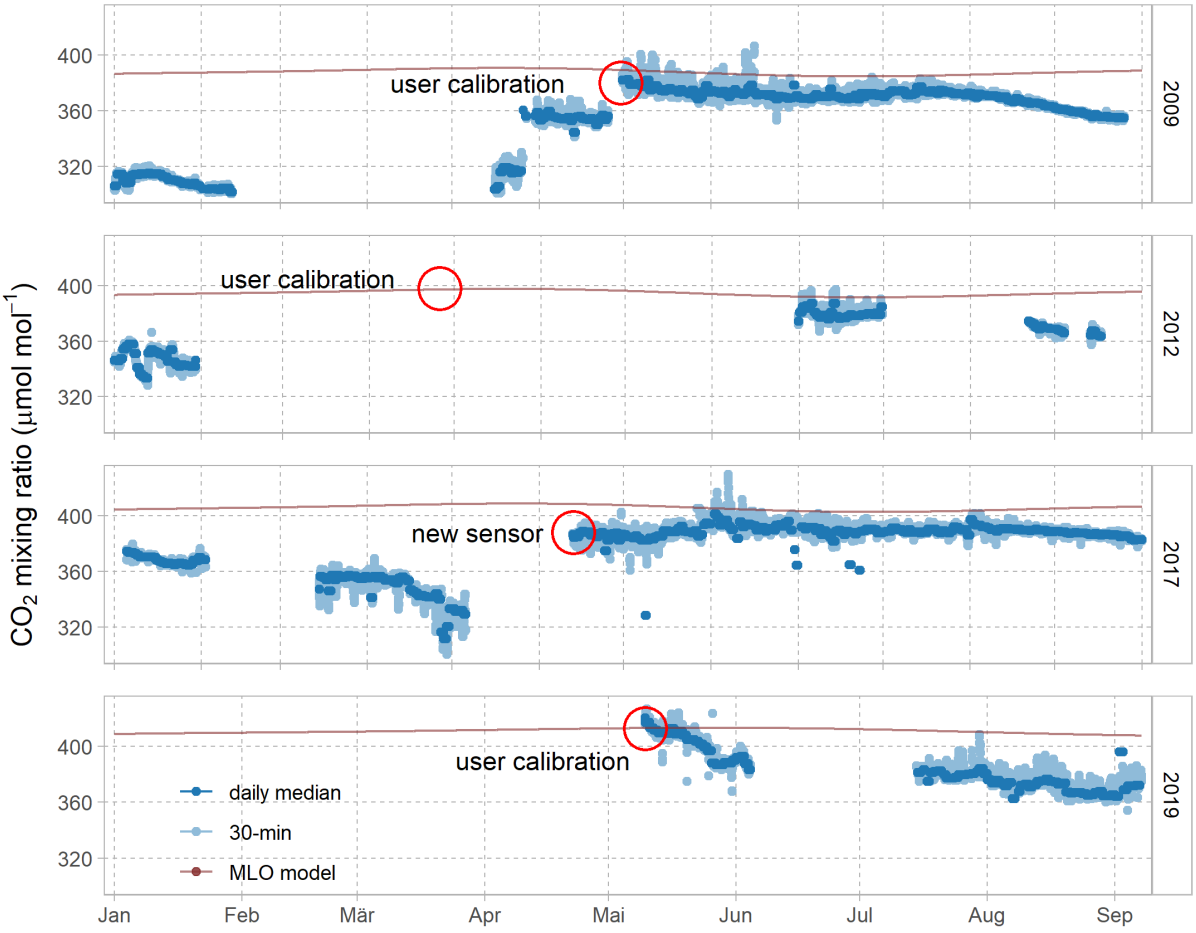

Fig. 4: CO2 mixing ratios during times with calibration

However, we agree with the reviewer that using the background concentration of Mauna Loa, which is at a distance of more than 11,000 km from our site, is unfavorable. We have tested our approach with the CO2 concentration data from Mt. Waliguan (Dlugokencky et al., 2020), which is at a distance of only about 1100 km from our study site, still on the Tibetan Plateau. We agree with the reviewer, that the measurements from this site probably better reflect the local background CO2 concentration at Nam Co. Figure 5 shows that there is a good agreement between the two time series, with the one from Mt. Waliguan exhibiting a more pronounced annual variation, with earlier minimum and maximum concentrations. This is probably due to the fact that Mt. Waliguan is situated right within the continental biosphere, rather than in the middle of an ocean. In order to generate a CO2 concentration time series with a 30-minute resolution we used the same approach as for the Mauna Loa data and fitted the model discussed above to monthly averages of the weekly flask measurements from Mt. Waliguan. The drift correction was re-calculated with the new CO2 reference and all subsequent flux calculations are now based on this data. The sections in the manuscript are updated accordingly and the model for the derivation of a 30-minute reference time series from observatory data is introduced and discussed.

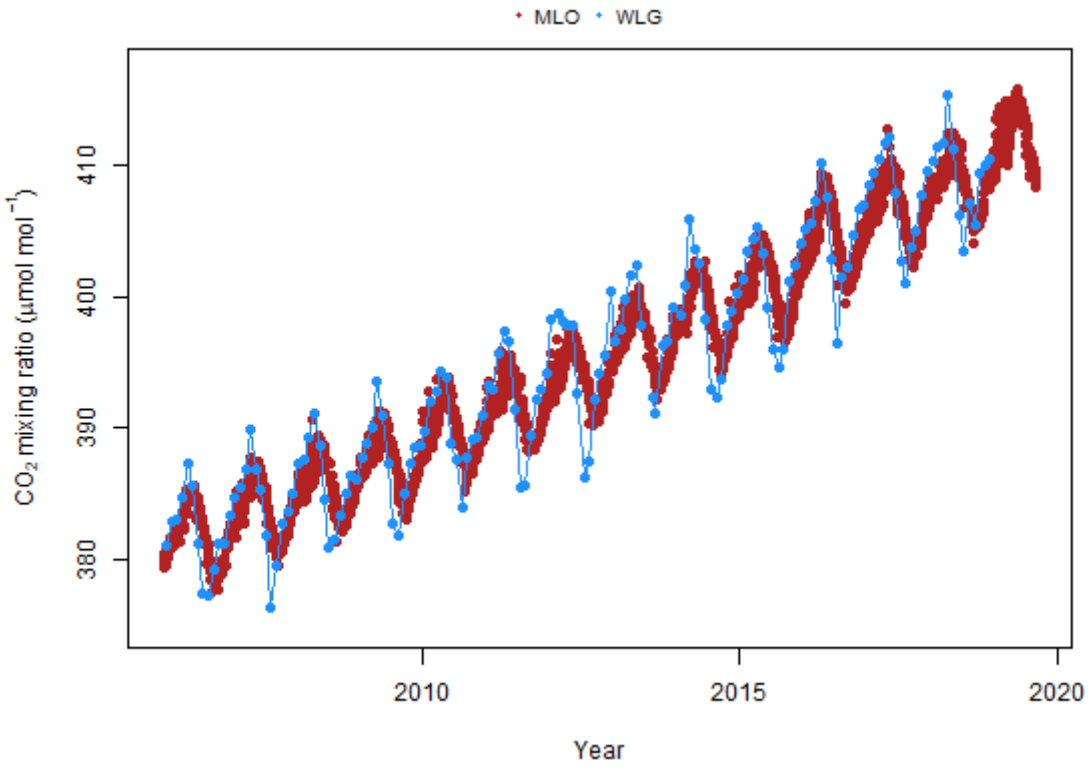

Fig. 5: CO2 concentration time series from Mauna Loa (red, daily average in-situ samples) and Mt. Waliguan (blue, weekly flask samples) atmospheric observatories.

3.3 Why not use the AGC to discard fluxes with dirty windows?

The AGC is a (loose) proxy for contamination, which is exactly what we address with the drift correction. The drift correction legitimately allows us to recover data with high AGC. Hence, we explicitly do not apply a general AGC filtering to the data set. Of course, when the AGC value rises above a certain level, the uncertainty in the signal is stronger so the overall quality of the drift correction could be degraded. We will add the AGC to the revised data set so that it may be used for further analyses.

3.4 Why does the qc scheme not efficiently remove the 612 data points with co2_mixing_ratio close to zero?

This problem is most probably a bug in the EddyPro software implementation. There are several arguments that hint in that direction: (1) The zeros (or close to zero) occur only in the co2_mixing_ratio. The values for co2_molar_density, co2_mole_fraction and co2_flux seem fine. (2) The corrupted co2_mixing_ratio occurs exactly every first entry after there was a data gap in the H2O reference concentration (possibly due to missing low frequency measurements). And indeed, when looking at the high frequency h2o_molar_density_li7500 we also see corrupted values every first entry after there was a data gap in the low frequency reference time series. Because the conversion from molar density to mixing ratio (of CO2 and H2O) depends on the h2o_molar_density, the corrupted values stem indeed from a software bug. The software implementation of the drift correction is still in development and was not yet officially released (i.e. you cannot use it via the GUI). A notification to fix the bug was filed and a fix will probably be implemented in one of the upcoming releases. Meanwhile, we removed erroneous CO2 and H2O mixing ratios manually by setting plausibility boundaries and added a short notice in Sect. 2.4. We are confident that our work around is appropriate

because the Li-7500 (as an open path instrument) anyway measures gas concentration in molar density first and calculates mole fraction and mixing ratio only afterwards. Hence, the calculated fluxes are not affected and can be used for analyses.

Changes in the manuscript concerning comment 3.1: No changes have been made in the manuscript.

Changes in the manuscript concerning comment 3.2: We replaced the Mauna Loa reference time series with the time series from Mt. Waliguan throughout the manuscript.

In the Methods Sect. 2.3 *Drift correction* we added information about the use of Mt. Waliguan as a reference time series and introduce the model used to derive the CO2 concentration offset: "[…] we used the CO2 mixing ratio measurements from Mt. Waliguan atmospheric observatory (years 2005-2018, Dlugokencky et al., 2020), situated approximately 1100 km NE of Nam Co, still on the Tibetan Plateau. We averaged the weekly flask measurements to monthly means and fitted the following model to the data:

$$CO_{2\,ref} = p_1 + p_2*t + p_3*\cos(2*\pi*t/365) + p_4*\sin(2*\pi*t/365) + p_5*\cos(4*\pi*t/365) + p_6*\sin(4*\pi*t/365),$$

where t is the decimal time in days and p_i are the fit parameters. This model was used to generate the 30-minute CO2 concentration reference time series. The rationale for using this model rather than a linear or spline interpolation was to mimic the general pattern of the atmospheric CO2 background concentration while excluding short term CO2 variations which most likely do not affect the Mt. Waliguan observatory and our site at the same time. We then calculated the CO2 offset used for the drift correction on a daily basis, as the difference between the daily medians of the measured CO2 concentration and the reference CO2 concentration. Hence, one offset value was applied to all 30-minute CO2 concentration measurements of each individual day. In contrast, the H2O offset was determined as the difference between the 30-minute H2O concentration measured by the Li-7500 gas analyzer and the H2O concentration calculated from auxiliary low frequency measurements of relative humidity, temperature and air pressure. The time series of 30 minute concentration offset values were imported as dynamic metadata file in EddyPro. Together with the sensor specific calibration information […]."

In the Sect. 4 *Discussion* we now discuss the uncertainty resulting from the use of a reference time series: "To be more precise on that, the measured daily medians remain approximately 10-15 ppm lower than the model right after user calibration was performed. An underestimation of 15 ppm around 400 ppm means about 3.75 % error in concentration, which leads to roughly 1.5 % error in flux for CO2 (the % error in flux is roughly 40 % of the % error in concentration, Fratini et al., 2014). Considering that the measured concentrations are often 100 to several 100 ppm away from the (assumed) real concentration and that this causes great errors in the raw flux and the WPL correction, this correction can be assumed to greatly reduce these errors. As seen in Figs. 3 and 4, after drift correction, the mean CO2 and H2O concentrations are very close to the (assumed) values. So even though not completely accurate, this strategy is expected to at least reduce the inaccuracy of the computed fluxes."

Changes in the manuscript concerning comment 3.3: No changes have been made in the manuscript.

Changes in the manuscript concerning comment 3.4: In the Results Sect. 3.1 *Drift correction* we added information about the software bug and its implications: "However, the software implementation of the drift correction is still in development and was not yet officially released (i.e. you cannot use it via the GUI), so unfortunately it still contains a software error (bug): Every data gap in the H2O reference concentration time series (due to e.g. missing low frequency meteorological data) produces a corrupted H2O mixing ratio record in the following half hour, which also affects the calculation of the

CO_2 mixing ratio. This issue was raised with the EddyPro developers and will be fixed in one of the upcoming releases. Because this error does not affect the calculation of the fluxes or other variables, we removed the erroneous values by setting plausibility limits."

H2O concentration:

Reviewer comment 4: The H2O concentrations provided in the data-file are not the once from the LI7500 but the once from the biomet data, i.e. the temperature and relative humidity sensor. This might be okay for a normal data set where no issues are present with drifts, dirty windows, concentration etc. But here I would highly recommend to provide or at least look at the water vapor concentration of the LI7500. When you use EddyPro for processing I think the only way to get the true LI7500 H2O concentrations is when you run the processing without providing the biomet file. The point here is that you can't use the concentration as a quality criteria. You can actually see that by looking at the number of qc_co2_mixing_ratio_composite and qc_h20_mixing_ratio_composite. The number of bad data for qc_co2_mixing_ratio_composite (==2) is 12730 and for qc_h2o_mixing_ratio_composite (==2) is 203. If the concentration of the one is bad usually also the other one is bad. Especially when this is due to dirty windows, precipitation, snow frost, etc… I really encourage you to use the real LI7500 water vapor concentrations to select a criterion to remove bad data and also bad fluxes of h2o. In principle I would recommend to provide the raw CO2 and H2O concentrations and the corrected once.

Response to reviewer comment 4: We agree with the reviewer that the mean H2O concentrations of the Li-7500 should be included in the data set. The Li-7500 H2O data can be taken from the EddyPro statistics output files. In the updated data set, all CO2 and H2O concentrations involved in the processing of the data set – non-drift corrected and drift corrected CO2 and H2O high frequency, as well as H2O low frequency concentrations – are included. Furthermore, we agree with the reviewer that the H2O concentration QC flag must be derived from the corrected high frequency H2O concentration signal. This is corrected in the updated data set, so that the same QC scheme is applied for H2O (low and high frequency) as for the CO2 gas concentration data. Please note that the gas concentrations are also used during the SSH correction. For the approach of Burba et al. (2008), EddyPro uses the quality filtered H2O data from the slow meteorological probe rather than the high frequency data from the Li-7500. To be consistent, we also used H2O data from the slow meteorological probe for the SSH approach of Frank and Massman (2020). An explanatory text was added to Sect. 2.4, 2.5 and also to the data description file.

Changes in the manuscript concerning comment 4: In the Methods Sect. 2.4 *Quality filtering* we included the following section: "Please note that the H2O gas densities and concentrations in the EddyPro full output file are calculated mainly from low frequency measurements of air temperature, pressure and relative humidity, probably because these are deemed more accurate than the high frequency measurements of the IRGA. To enhance comparability, we extracted the high frequency H2O gas densities from the EddyPro statistics output file (variable 'mean(h2o)') and calculated the mole fraction and mixing ratio. These variables were quality filtered following the same scheme as above and are supplied with the data set (suffix: _Li7500)."

In the Methods Sect. 2.5 *Sensor self heating correction* we added the following note: "Please note that we used the quality filtered variable co2_molar_density from the EddyPro full output file in order to reproduce the calculations."

Minor comments:

Reviewer Comment 5: Please include the countries to which the southern and western part of the TP belongs. I guess Nepal, Pakistan, India and Bhutan.

Response to reviewer comment 5: Thanks for the suggestion, the names of neighboring countries have been included in the text.

Changes in the manuscript concerning comment 5: The respective sentence in the introduction was rephrased: "It has an area of about 2.5 million km^2 at an average elevation of > 4000 m above sea level and includes the entire southwestern Chinese provinces of Tibet and Qinghai, parts of Gansu, Yunnan, Sichuan, as well as parts of India, Nepal, Bhutan and Pakistan."

Reviewer Comment 6: The sine-cosine model is not explained. Why not directly using a spline function or even a moving average? Did you use the flask samples or the continuous? The pattern of the CO2 concentrations is not really a sine or cosine.

Response to reviewer comment 6: We explained the model and the rationale behind it under the point 3.2. above.

Changes in the manuscript concerning comment 6: Please see point "Changes in the manuscript concerning comment 3.2" above.

Reviewer Comment 7: I think the u* filtering should be applied. Just because there s wind does not mean there is no relationship. For grassland values around u* values of 0.1 m/s are not so uncommon and that accounts in your data set for 15% of all u* values. The red line in the plot shows the cumulated density function multiplied by 3000 to fit the scale. Green vertical line is at u*== 0.1 m/s.

Response to reviewer comment 7: We agree with the reviewer and added u* filtering to our processing pipeline. We think that one overall u* threshold is sufficient because vegetation height remains very low throughout the year. The threshold was estimated using REddyProc. We added a quality flag (qc_ustar), indicating whether a 30-min flux has a lower u* than the estimated threshold. These were then excluded from further analyses. A short paragraph was added to the text and in the data description file.

Changes in the manuscript concerning comment 7: We added the following text to Sect. 2.4 *Quality filtering*: "To identify periods with insufficient turbulent mixing, we estimated the friction velocity (u*) threshold using the REddyProc R package. Fluxes with u* < 0.08 m s^{-1} were excluded from subsequent calculations."

Furthermore, Table A1 now includes the proportion of available fluxes after u* filtering and a quality flag (qc_ustar) was added to the data set and to the data description file.

Reviewer Comment 8: Formular 7 and 8 you use mu and sigma which are usually the population mean and its standard deviation. I know you took it from the paper of Burba but there are plenty of other variables one can use. For the uncertainty analysis of the WPL I have only a gut feeling that this is wrong but it would be good if you would get some statisticians input and explain why this is valid to

do. In principle each value n the formula has an uncertainty e.g. Ta which propagates in Cp and rho. Sorry for not being more helpful on this one. But generally, for the overall uncertainty I would rather take the NEE_fsd to calculate the uncertainty of the fluxes. It is including not only the random error but also temporal variability and spatial heterogeneity. There is a paper comparing these uncertainties with each other I think in a savanna (sorry I can't recall the author maybe worth a look).

Response to reviewer comment 8: We revised the error propagation section. We now agree with the reviewer that that the error propagation calculation is not adequate, mostly due to the fact that the errors in the fluxes involved (H, LE, CO2) are not statistically independent of each other. Hence the standard error propagation method cannot be applied and has to be discarded. In the updated data set, we rely on the random flux uncertainties calculated by EddyPro following Finkelstein and Sims (2001). These should sufficiently cover the flux uncertainty that originates due to the sampling errors.

Additionally, the standard deviation of the marginal distribution sampling (MDS) gap-filling procedure (Reichstein et al., 2005) can be used as a measure for flux uncertainty. In the "savanna" paper mentioned by the reviewer, El-Madany et al. (2018), compared the random flux uncertainty (Finkelstein and Sims, 2001), the standard deviation of the marginal distribution sampling (MDS) gap-filling procedure (Reichstein et al., 2005), and a Two-Tower uncertainty (Hollinger and Richardson, 2005) from three different towers in the same ecosystem (but with non-overlapping footprints). As we only have one flux tower, we cannot apply the two-tower uncertainty but the standard deviation of the MDS gap-filling (NEE_fsd) is included in the data set. The NEE values for gap filling are (mostly) calculated using a look-up table approach with quite narrow meteorological bins (bin width: Rg = 5 W m^{-2}, VPD = 5 hPa, Tair = 2.5 °C) within a short time window (+- 7 days). During these conditions, the vegetation should not change a lot and hence, the ecosystem response to atmospheric drivers should be the same. Any variability of the flux measurements probably stems from the temporal (+- 7 days sampling window) and spatial (changes in footprints between 30-min fluxes) heterogeneity at the site. Hence, we could use the NEE_fsd as an additional measure for flux uncertainty to complement the random uncertainty estimation of Finkelstein and Sims (2001). As expected, the random uncertainty remains much lower than the NEE_fsd (medians of 0.2 and 0.5 µmol m^{-2} s^{-1}, respectively, Fig. 6).

Changes in the manuscript concerning comment 8: The random flux error propagation via the WPL correction was removed throughout the manuscript.

In Sect. 2.7 *Flux uncertainty estimation* we added the following text describing the rationale behind the use of NEE_fsd as a flux uncertainty estimate: "Because the RE method is based on the half hourly auto- and cross-correlation of the vertical wind component and the scalar of interest (e.g. air temperature or gas concentration), it contains only very limited information about spatial, temporal or meteorological variability (El-Madany et al., 2018). During the MDS gap filling procedure (Reichstein et al., 2005), the missing NEE values are (mostly) calculated using a look-up table approach with quite narrow meteorological bins (bin width: Rg = 5 W m^{-2}, VPD = 5 hPa, Tair = 2.5 °C) within a short time window (+/- 7 days). During these conditions, the vegetation should not change a lot and hence, the ecosystem response to atmospheric drivers should remain the same. Any variability of the flux measurements probably stems from the temporal (+/- 7 days sampling window) and spatial (changes in footprints between 30-min fluxes) heterogeneity at the site. Hence, we could use the standard deviation of the fluxes used for gap filling (NEE_fsd) as an additional measure for flux uncertainty to complement the random uncertainty estimation of Finkelstein and Sims (2001)"

We added an additional Fig. 8 which shows the monthly mean diurnal course and the annual course of the daily mean of the CO2 flux and uncertainty estimates (RE and NEE_fsd):

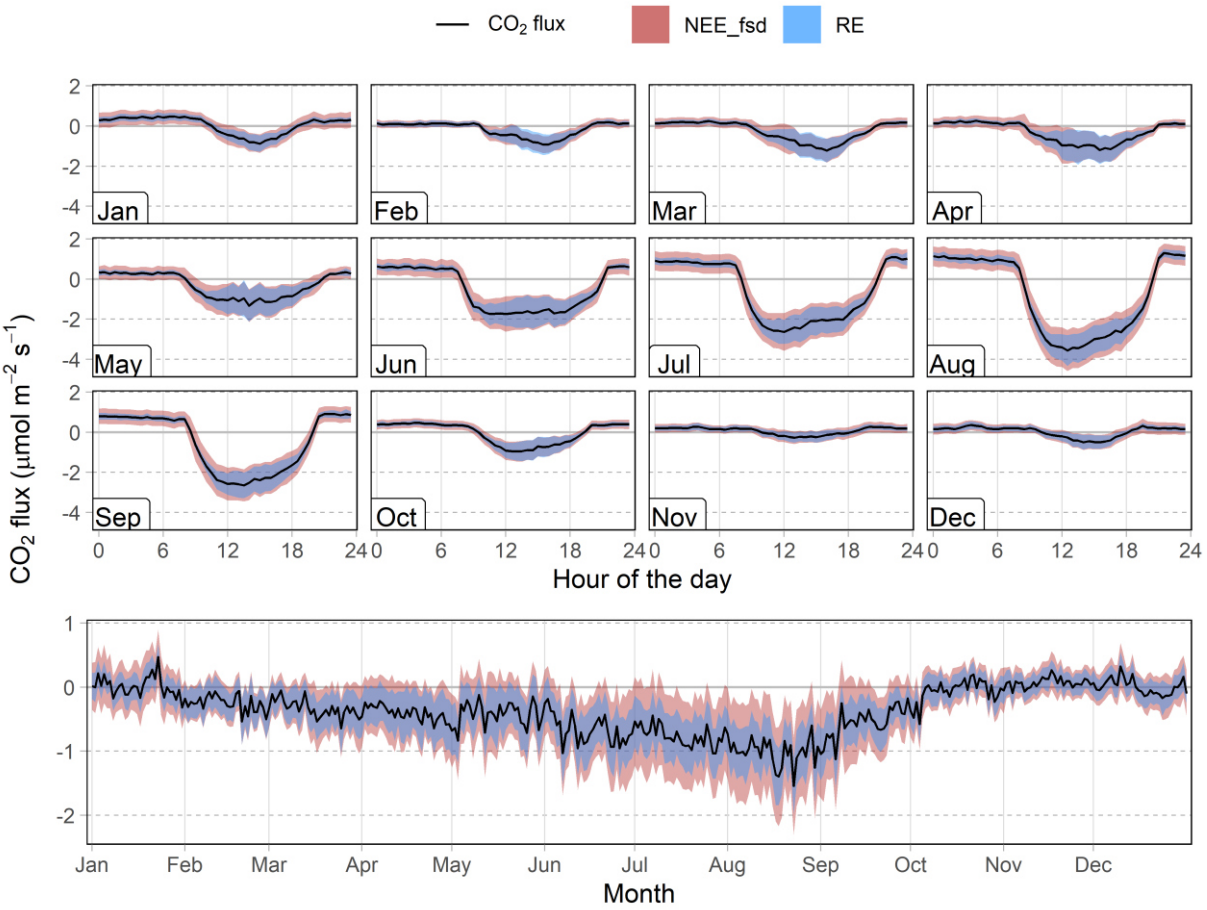

Fig. 6: The new Fig. 8 in the manuscript: Monthly mean diurnal course and annual course of daily mean of the CO2 flux and uncertainty estimates: RE is the random uncertainty following Finkelstein and Sims (2001), NEE_fsd is the standard deviation of values used for gap filling after Reichstein et al. (2005).

Furthermore, we added a new Results Section 3.4 *Flux uncertainty estimation* describing the results of the uncertainty estimation and describing the new Fig. 8: "Figure 8 shows the mean diurnal and annual cycle of the CO2 flux and the respective uncertainties. The two uncertainty estimates (RE, NEE_fsd) follow a distinct distribution, thereby reflecting the different sources of error they represent. As expected, the random uncertainty remains much lower than the standard deviation of the gap-filled fluxes (medians of 0.2 and 0.5 µmol m^{-2} s^{-1}, respectively). The RE exhibits roughly the same magnitude throughout the year whereas the NEE_fsd increases with increasing flux magnitude. Concerning the diurnal course, we see lower uncertainties during nighttime and winter than during daytime and summer. The RE is generally smaller during night while during daytime, the uncertainties almost converge."

In the Sect. 4 *Discussion* a sentence was added to describe which uncertainties are covered by our estimates: "The random uncertainty estimates described above represent random flux components as well as spatial heterogeneity, temporal variability, and small meteorological variability while neglecting other sources of random flux errors such as instrument noise."

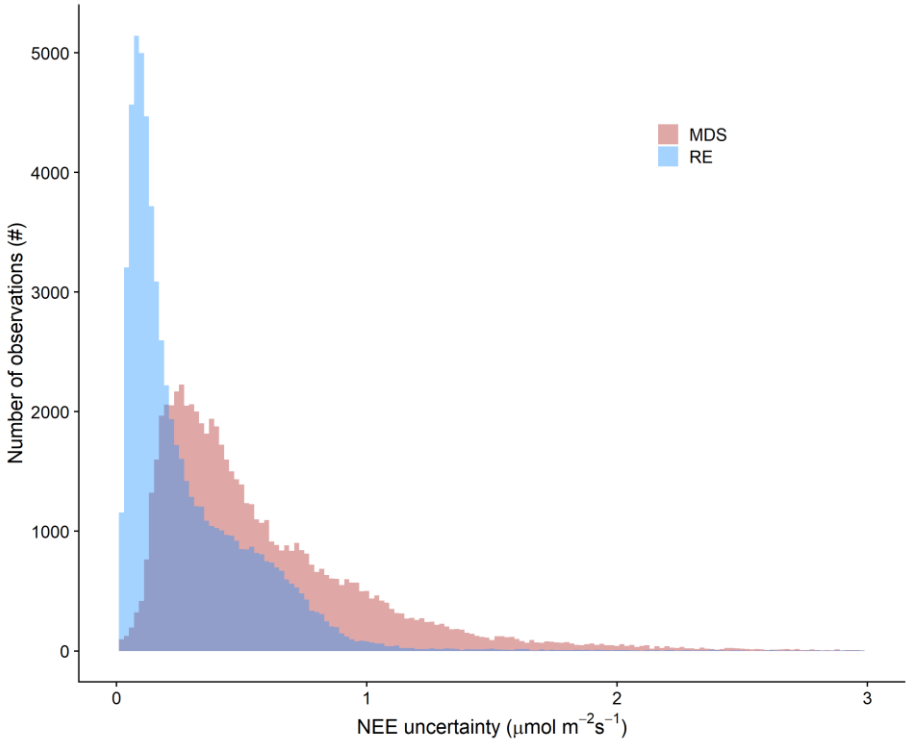

Fig. 7: Histograms of two different CO2 flux uncertainties. MDS is the standard deviation of the gap-filling procedure after Reichstein et al. (2005) and RE is the random uncertainty estimate following Finkelstein and Sims (2001).

Reviewer Comment 9: The sentence in line 425 "The wind direction distributions of wind speed and TKE, as well as the analysis of cumulative footprints suggest that the several buildings which were constructed in close vicinity of the tower do exert some influence on the flow regime while not violating basic EC assumptions. Nevertheless, fluxes originating mainly from the disturbed areas should be excluded from further analyses as they may be compromised by human activities." You have all indications that the flow was clearly disturbed and you still conclude that the assumptions of eddy covariance are met? How does that go together?

Response to reviewer comment 9: The statement, that basic EC assumptions are not violated was made with respect to the fulfillment of SS and ITC tests. Basically meaning, that the values are not usable, although qc_co2_flux == 0 and should hence be excluded from further analyses, as we state correctly in the subsequent sentence. We agree that the sentence is unclear so we changed the formulation to avoid confusion about this.

Changes in the manuscript concerning comment 9: The respective sentence in the Sect. 5 *Conclusions* was changed: "The wind direction distributions of wind speed and TKE suggest that the several buildings which were constructed in close vicinity of the tower do exert some influence on the flow regime. Fluxes originating from the disturbed areas should be excluded from further analyses as they may be compromised by human activities."

Reviewer Comment 10: For the data description file some more info on the uncertainties would be great. The differences are not directly clear to the reader.

Response to reviewer comment 10: The variables “rand_err_co2_flux_wpl” and “rand_err_h2o_flux_wpl” are not calculated anymore so they had to be removed from the data description file. Concerning “rand_err_co2_flux” and “rand_err_h2o_flux”, information about the calculation method was added to the data description file.

Changes in the manuscript concerning comment 10: No changes have been made in the manuscript. In the data description file we added a short statement after which method (Finkelstein and Sims, 2001) the random error was calculated.

Additional changes made by the authors:

We added the DOI and source of the second data set repository (National Tibetan Plateau Data Center) in the abstract.

In the Methods Sect. 2.4 *Quality filtering* we stated that we filtered for discontinuities while in fact we did not use this measure. We corrected the formulation accordingly.

During gap filling, we additionally filtered for night time fluxes < -0.1 µmol m^{-2} s^{-1} and excluded the upper and lower 0.2 % in order to exclude implausible fluxes from the gap-filling procedure. We added a note in the Methods Sect 2.6 *Gap filling*: "Prior to the processing, we excluded the lower and upper 0.2 % of the fluxes and discarded physiological implausible night time fluxes < -0.1 µmol m^{-2} s^{-1}."

We introduced the following figure showing the offset between the Li-7500 H2O concentration measurements and the low frequency reference time series before and after drift correction. This should help to illustrate the effect of the drift correction procedure.

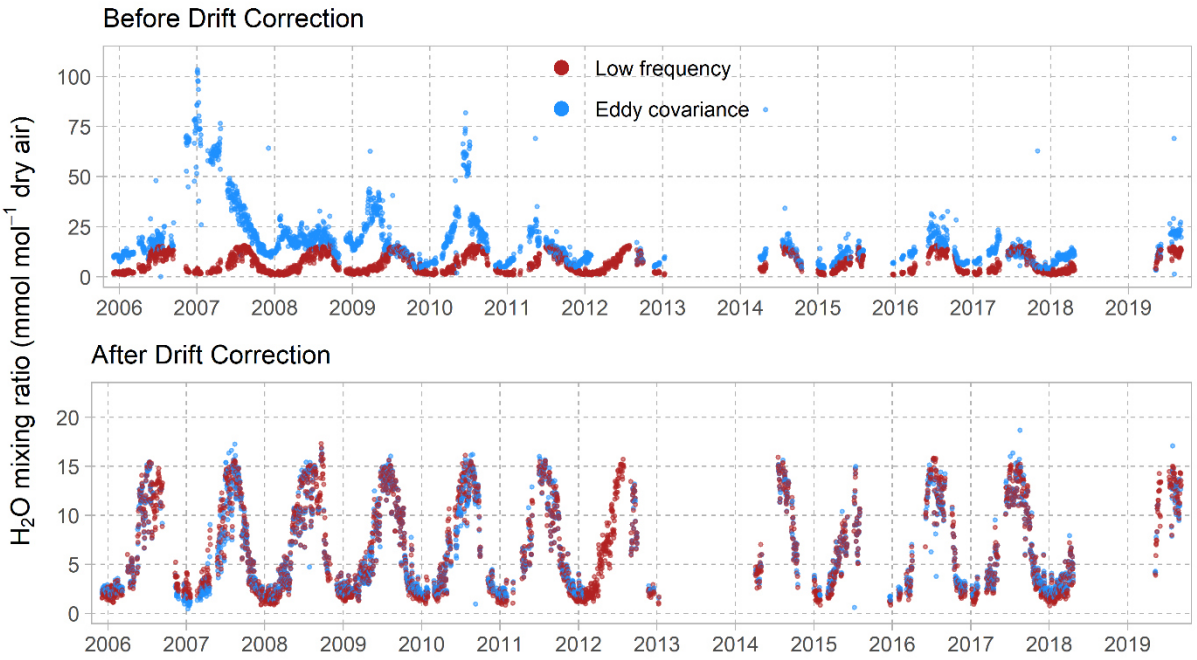

Figure 8: The new Fig. 4. In the manuscript: Half hourly H2O dry air mixing ratios and low frequency reference concentration before and after drift correction. H2O mixing ratios have been checked for repeating values and outliers using the same algorithms as in Sect. 2.4. Please note the different y-axis scales.

References:

Bate, G. C. and Smith, V. R.: Photosynthesis and respiration in the Sub-Antarctic tussock grass Poa cookii, The New phytologist, 95, 533–543, doi:10.1111/j.1469-8137.1983.tb03518.x, 1983.

Burba, G. G., McDermitt, D. K., Grelle, A., Anderson, D., and XU, L.: Addressing the influence of instrument surface heat exchange on the measurements of CO 2 flux from open-path gas analyzers, Glob Change Biol, 14, 1854–1876, doi:10.1111/j.1365-2486.2008.01606.x, 2008.

Dlugokencky, E. J., Mund, J. W., Crotwell, A. M., Crotwell, M. J., and Thoning, K. W.: Atmospheric Carbon Dioxide Dry Air Mole Fractions from the NOAA GML Carbon Cycle Cooperative Global Air Sampling Network, 1968-2019: Version: 2020-07, doi:10.15138/wkgj-f215, 2020.

El-Madany, T. S., Reichstein, M., Perez-Priego, O., Carrara, A., Moreno, G., Pilar Martín, M., Pacheco-Labrador, J., Wohlfahrt, G., Nieto, H., Weber, U., Kolle, O., Luo, Y.-P., Carvalhais, N., and Migliavacca, M.: Drivers of spatio-temporal variability of carbon dioxide and energy fluxes in a Mediterranean savanna ecosystem, Agricultural and Forest Meteorology, 262, 258–278, doi:10.1016/j.agrformet.2018.07.010, 2018.

Finkelstein, P. L. and Sims, P. F.: Sampling error in eddy correlation flux measurements, J. Geophys. Res. Atmos., 106, 3503–3509, doi:10.1029/2000JD900731, 2001.

Frank, J. M. and Massman, W. J.: A new perspective on the open-path infrared gas analyzer self-heating correction, Agricultural and Forest Meteorology, 290, 107986, doi:10.1016/j.agrformet.2020.107986, 2020.

Fratini, G., McDermitt, D. K., and Papale, D.: Eddy-covariance flux errors due to biases in gas concentration measurements: origins, quantification and correction, Biogeosciences, 11, 1037–1051, doi:10.5194/bg-11-1037-2014, 2014.

Hollinger, D. Y. and Richardson, A. D.: Uncertainty in eddy covariance measurements and its application to physiological models, Tree physiology, 25, 873–885, doi:10.1093/treephys/25.7.873, 2005.

Kappen, L., Schroeter, B., Scheidegger, C., Sommerkorn, M., and Hestmark, G.: Cold resistance and metabolic activity of lichens below 0°C, Advances in Space Research, 18, 119–128, doi:10.1016/0273-1177(96)00007-5, 1996.

Kittler, F., Eugster, W., Foken, T., Heimann, M., Kolle, O., and Göckede, M.: High-quality eddy-covariance CO 2 budgets under cold climate conditions, J. Geophys. Res. Biogeosci., 122, 2064–2084, doi:10.1002/2017JG003830, 2017.

Miller, L. A., Papakyriakou, T. N., Collins, R. E., Deming, J. W., Ehn, J. K., Macdonald, R. W., Mucci, A., Owens, O., Raudsepp, M., and Sutherland, N.: Carbon dynamics in sea ice: A winter flux time series, J. Geophys. Res., 116, doi:10.1029/2009JC006058, 2011.

Oechel, W. C., Laskowski, C. A., Burba, G., Gioli, B., and Kalhori, A. A. M.: Annual patterns and budget of CO 2 flux in an Arctic tussock tundra ecosystem, J. Geophys. Res. Biogeosci., 119, 323–339, doi:10.1002/2013JG002431, 2014.

Reichstein, M., Falge, E., Baldocchi, D., Papale, D., Aubinet, M., Berbigier, P., Bernhofer, C., Buchmann, N., Gilmanov, T., Granier, A., Grunwald, T., Havrankova, K., Ilvesniemi, H., Janous, D., Knohl, A., Laurila, T., Lohila, A., Loustau, D., Matteucci, G., Meyers, T., miglietta, F., ourcival, J.-m., Pumpanen, J., Rambal, S., Rotenberg, E., Sanz, M., Tenhunen, J., Seufert, G., Vaccari, F., Vesala, T., Yakir, D., and valentini, R.: On the separation of net ecosystem exchange into assimilation and ecosystem respiration: review and improved algorithm, Glob Change Biol, 11, 1424–1439, doi:10.1111/j.1365-2486.2005.001002.x, 2005.

Sabbatini, S., Mammarella, I., Arriga, N., Fratini, G., Graf, A., Hörtnagl, L., Ibrom, A., Longdoz, B., Mauder, M., Merbold, L., Metzger, S., Montagnani, L., Pitacco, A., Rebmann, C., Sedlák, P., Šigut, L., Vitale, D., and Papale, D.: Eddy covariance raw data processing for CO2 and energy fluxes calculation at ICOS ecosystem stations, International Agrophysics, 32, 495–515, doi:10.1515/intag-2017-0043, 2018.

Webb, E. E., Schuur, E. A. G., Natali, S. M., Oken, K. L., Bracho, R., Krapek, J. P., Risk, D., and Nickerson, N. R.: Increased wintertime CO 2 loss as a result of sustained tundra warming, J. Geophys. Res. Biogeosci., 121, 249–265, doi:10.1002/2014JG002795, 2016.

A Long Term (2005 - 2019) Eddy Covariance Data Set of CO_2 and H_2O Fluxes from the Tibetan Alpine Steppe

Felix Nieberding[1,2], Christian Wille[2], Gerardo Fratini[3], Magnus O. Asmussen[1], Yuyang Wang[4,5,6], Yaoming Ma[4,5,6], and Torsten Sachs[2,1]

[1]Technische Universität Braunschweig, Germany
[2]GFZ German Research Centre for Geosciences, Potsdam, Germany
[3]LI-COR Biosciences Inc., Lincoln, Nebraska, USA
[4]Key Laboratory of Tibetan Environment Changes and Land Surface Processes, Institute of Tibetan Plateau Research, Chinese Academy of Sciences, Beijing, China
[5]CAS Center for Excellence in Tibetan Plateau Earth Sciences, Beijing, China
[6]University of Chinese Academy of Sciences, Beijing, China

Correspondence: Felix Nieberding (f.nieberding@tu-braunschweig.de), Yaoming Ma (ymma@itpcas.ac.cn)

Abstract. The Tibetan alpine steppe ecosystem covers an area of roughly 800,000 km^2, containing up to 3.3 % soil organic carbon in the uppermost 30 cm, summing up to 1.93 Pg C for the Tibet Autonomous Region only (472,037 km^2). With temperatures rising two to three times faster than the global average, these carbon stocks are at risk of loss due to enhanced soil respiration. The remote location and the harsh environmental conditions on the Tibetan Plateau (TP) make it challenging to derive accurate data on ecosystem-atmosphere exchange of carbon dioxide (CO_2) and water vapor (H_2O). Here, we provide the first multi-year data set of CO_2 and H_2O fluxes from the central Tibetan alpine steppe ecosystem, measured in situ using the eddy covariance technique. The calculated fluxes were rigorously quality checked and carefully corrected for a drift in concentration measurements~~and~~. The gas analyzer self heating effect during cold conditions was evaluated using the standard correction procedure and newly revised formulations (Burba et al., 2008; Frank and Massman, 2020). A wind field analysis was conducted to identify influences of adjacent buildings on the turbulence regime and to exclude the disturbed fluxes from subsequent computations. The presented CO_2 fluxes were additionally gap filled using a standardized approach. The very low net carbon uptake across the 15-year data set highlights the special vulnerability of the Tibetan alpine steppe ecosystem to become a source of CO_2 due to global warming. The data is freely available ~~(https://www.doi.org/10.5281/zenodo.3733203, Nieberding et al., 2020b) and~~ under https://www.doi.org/10.5281/zenodo.3733202 (Nieberding et al., 2020a) and https://doi.org/10.11888/Meteoro.tpdc.270333 (Nieberding et al., 2020b) and may help to better understand the role of the Tibetan alpine steppe in the global carbon-climate feedback.

1 Introduction

The Tibetan Plateau is also called "The Third Pole" because it harbors the third largest ice mass on earth, right after the polar regions (Qiu, 2008). It has an area of about 2.5 million km^2 at an average elevation of > 4000 m above sea level and includes the entire southwestern Chinese provinces of Tibet and Qinghai, parts of Gansu, Yunnan, Sichuan~~and neighboring countries~~, as well as parts of India, Nepal, Bhutan and Pakistan. Similarly to the northern high latitudes, the TP is warming considerably faster than the global average, with air temperatures rising at a rate of 0.35 K per decade (from 1970 to 2014) (Yao et al., 2019). At the same time, the TP is experiencing changes in precipitation rates, which alter its water cycle, possibly affecting 1.65 billion people across South East Asia (Cuo and Zhang, 2017). While precipitation is reduced on the southern and eastern margins of the TP, it is enhanced in the central area, partly due to higher temperatures and thus enhanced evaporation, leading to more effective water recycling (Yang et al., 2014; Wang et al., 2018). The majority of the TP is covered by the biggest ~~pastoralist~~ pastural system in the world, the so called steppe-meadow ecotone, consisting of 450,000 km^2 *Kobresia* (syn. *Carex*) *pygmaea* pastures and 800,000 km^2 alpine steppe ecosystem (Miehe et al., 2011, 2019). With decreasing precipitation to the west, the *K. pygmaea* pastures are replaced by alpine steppe ecosystems. With 14-48 % mean total vegetation cover, the alpine steppe exhibits considerably less above-ground biomass than the *K. pygmaea* pastures. At least in the eastern part, the alpine steppe soils still contain an almost 30 cm thick, ~~organically rich~~ organic-rich layer, which consists of up to 3.3 % soil organic carbon (SOC), summing up to 1.93 Pg C for the Tibet Autonomous Region only (472,037 km^2) (Zhou et al., 2019). Hence, the response of CO_2 and H_2O fluxes to environmental changes in the Tibetan Plateau grasslands are crucial for the water cycling in greater Asia and the global carbon budget, respectively. While the carbon cycling in *Kobresia* pastures has been studied extensively, the alpine steppe ecosystem remains underrepresented, particularly with regard to long term observations.

This study presents nearly 15 years of eddy covariance data from an alpine steppe ecosystem on the central Tibetan Plateau. The aim of this study is to calculate consistent CO_2 fluxes while following standardized quality control methods to allow for comparability between the different years of our record and with other data sets. To ensure meaningful estimates of ecosystem-atmosphere exchange, careful application of the following correction procedures and analyses was necessary: (1) Due to the remote location, continuous maintenance of the ~~EC~~ eddy covariance (EC) system was not always possible, so that cleaning and calibration of the sensors was performed irregularly. Furthermore, the high proportion of bare soil and high wind speeds led to accumulation of dirt in the measurement path of the ~~IRGA~~infrared gas analyzer (IRGA). The installation of the sensor in such a challenging environment resulted in a considerable drift in CO_2 and H_2O gas density measurements. If not accounted for, this concentration bias may distort the estimation of the carbon uptake. We applied a modified drift correction procedure following Fratini et al. (2014) which, instead of a linear interpolation between calibration dates, uses the CO_2 concentration measurements from the ~~Mauna Loa~~ Mt. Waliguan atmospheric observatory as reference time series. (2) We applied rigorous ~~low frequency quality filtering~~ quality filtering of the calculated fluxes to retain only ~~flux measurements~~ fluxes which represent actual physical processes. (3) During the long measurement period, there were several buildings constructed in the near vicinity of the EC system. We investigated the influence of these obstacles on the turbulent flow regime ~~and conducted a footprint analysis~~ to identify fluxes with uncertain land cover contribution and exclude them from subsequent computations. (4) We ~~applied a~~

calculated the de-facto standard correction for instrument surface heating during cold conditions (hereafter called sensor self heating correction~~after Burba et al. (2008)) , following the approach of Oechel et al. (2014))~~ following Burba et al. (2008) and a revision of the original method following Frank and Massman (2020). (5) Subsequently, we applied the traditional and widely used gap filling procedure following Reichstein et al. (2005) to provide a more complete overview of the annual net ecosystem CO_2 exchange. (6) We estimated the ~~random uncertainty~~ flux uncertainty by calculating the random flux error (RE) following Finkelstein and Sims (2001) and ~~analyzed the error propagation through the WPL correction to get an estimation of the accuracy of the measurements~~by using the standard deviation of the fluxes used for gap filling (NEE_fsd) as a measure for spatial and temporal variation.

2 Material and methods

2.1 Site description and measurements

The Nam Co Station for Multi-sphere Observation and Research (NAMORS, Chinese Academy of Sciences) is located at 4730 m a.s.l., about 220 km north of the Tibetan capital Lhasa (30° 46' N, 90° 57' S; Fig. 1). It is situated on an almost flat plain between the ENE-WSW oriented Nyainqêntanglha range in 15 km distance to the SSE and lake Nam Co about 1 km to the NW. The climate at Nam Co is characterized by strong seasonality, with long, cold winters and short but moist summers. The mean annual air temperature measured at the NAMORS research station between 2005 and 2019 was -0.2 °C. During winter, the Westerlies control the general circulation and lead to cold and dry weather, with temperature minima below -20 °C. Although snow storms do occur during winter time, a closed snow cover is seldom reached for longer time periods. In springtime, the TP heats up and allows the melt water to percolate to deeper soil layers. The drought situation increases gradually until the monsoon rains arrive, typically between May and June. The southern branch of the westerlies needs to shift northward of the Tibetan Plateau so that the humid air masses from the intertropical convergence zone can reach the plateau along meridional river gorges, thus increasing precipitation notably. The annual precipitation ranges from 291 to 568 mm (mean = 403 mm), with the majority occurring during the monsoon season from May to October. During autumn, weather shifts again to clear, cold and dry conditions (Yao et al., 2013). The study site is covered by degraded *Stipa purpurea* alpine steppe vegetation, which includes species from the families *Artemisia*, *Stipa*, *Poa*, *Festuca* and *Carex* (Li et al., 2018; Miehe et al., 2011). The vegetation heights do not exceed 5 cm due to heavy grazing by yak and sheep and the plant cover is usually less than 50 % (Nölling, 2006). The substrate is mostly soil and loess. The (micro-) meteorological measurements at the NAMORS site were established in 2005 by the Institute of Tibetan Plateau Research (ITP), Chinese Academy of Sciences (CAS) (Ma et al., 2009). The measurement complex is comprised of a 52 m tall Planetary Boundary Layer (PBL) tower measuring air temperature and relative humidity in 5 different heights and wind speed and wind direction in 3 different heights (1.5 m, 2 m, 4 m, 10 m, 20 m and 1.5 m, 10 m, 20 m, respectively). The 3 m Eddy Covariance measurement tower is equipped with a ~~CSat3~~ CSAT3 ultrasonic anomometer (USA) and a Li-7500 open path infrared gas analyzer (IRGA). The separation between the two sensors is 23 cm. In June 2009, the sonic anemometer alignment was changed from 135 degrees to 200 degrees. In 2010, a KH50 krypton hygrometer was installed but the data is not available due to quality constraints. The site is further supplemented with

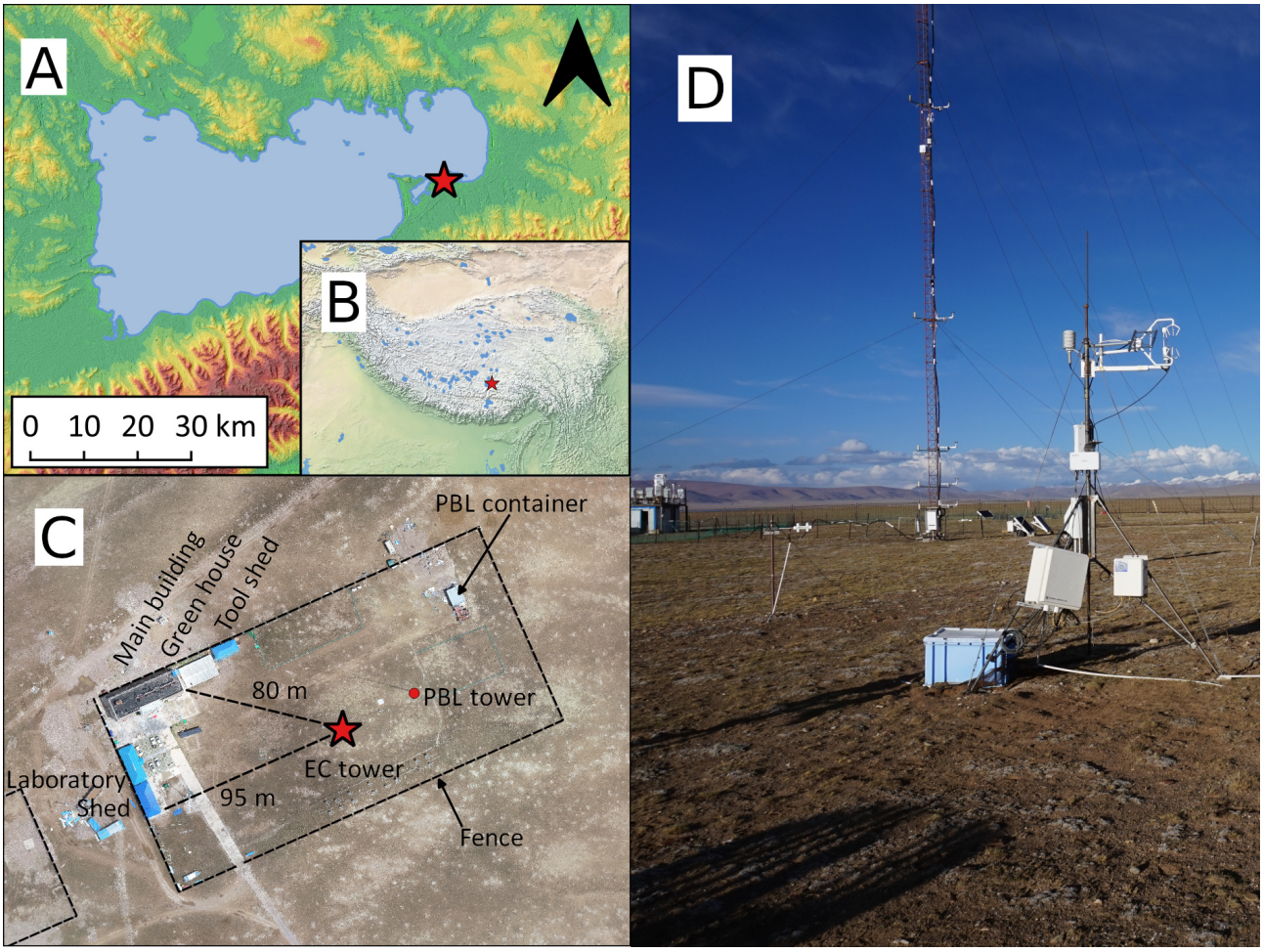

Figure 1. (A) Study site at the NAMORS station close to lake Nam Co (ASTER GDEM V3, NASA/METI/AIST/Japan Spacesystems, and U.S./Japan ASTER Science Team, 2019). (B) Overview map showing the location on the Tibetan Plateau, made with Natural Earth. (C) Aerial image of the NAMORS station with the main features in July 2019. Images by Guoshuai Zhang. (D) Photo of the EC system (front), PBL tower and part of the PBL container (back) in May 2019. Photo by Felix Nieberding.

measurements of soil moisture and soil temperature (0 cm, -10 cm, -20 cm, -40 cm, -80 cm, -160 cm), soil heat flux (-10 cm, -20 cm) and radiation (short and long wave downward and upward radiation, global radiation), precipitation and air pressure measurements. In 2013 the station was extended for a photosynthetic photon flux density sensor (PPFD) (Zhu et al., 2015). For detailed information about available measurements and sensor types please see Ma et al. (2009).

2.2 EC raw data processing

The Eddy Covariance method is a direct micrometeorological approach to estimate turbulent exchange of heat, momentum and matter between the atmosphere and the underlying surface (Aubinet et al., 2012). It is a common approach to estimate the net ecosystem CO_2 exchange (NEE), which is the sum of carbon uptake via photosynthesis of green vegetation (Gross Primary Production, hereafter GPP) and carbon release through autotrophic and heterotrophic respiration (Ecosystem Respiration, hereafter R_{eco}). The turbulence measurements were conducted with a ~~Csat3~~ CSAT3 ultrasonic anemometer measuring the three-dimensional wind vector. A Li-7500 infrared gas analyzer was placed in close vicinity to the anemometer, measuring the CO_2 concentration of the up- and downward moving air parcels. The acquisition frequency is 10 Hz and the fluxes were calculated for every 30-min interval using the raw data processing software EddyPro (v7.0.6, LI-COR Inc.). Table 1 shows the processing and correction procedure which follows standardized and well tested methods including despiking, axis rotation, detrending and data quality flagging based on stationarity, instrument performance, as well as integral turbulence characteristics (Foken and Wichura, 1996; Foken et al., 2004). The data flagging policy is following Mauder and Foken (2006), with "0" for high quality fluxes, "1" for intermediate quality fluxes and "2" for poor quality fluxes. Following the usual ~~atmospheric~~ meteorological convention, positive values represent fluxes moving away from the surface and negative values represent fluxes moving towards the surface. During 2006 and 2007 the sonic anemometer exhibited a step wise downward vertical tilt of up to 13 degrees. This was accounted for by calculating the planar fit coordinate rotation only for times when the orientation of the sonic anemometer remained constant. The dates were derived visually by analyzing the second rotation angle (pitch), estimated from a preliminary raw data processing using the double rotation method.

2.3 Drift correction

The Li-7500 is a so called "dual wavelength, single path" instrument that estimates CO_2 and water vapor density (ρ_c and ρ_v, respectively) from the amount of radiation passing an ambient air volume in a gas absorbing wavelength, relative to the amount of radiation passing the same sample volume in a non-absorbing reference wavelength. The absorbing wavelengths are 4.25 µm and 2.59 µm for CO_2 and H_2O, respectively, with both sharing the same non-absorbing reference wavelength of 3.95 µm (Serrano-Ortiz et al., 2008). Absorptance is then converted into an estimate of gas number density by means of an instrument specific curvilinear calibration curve. Due to small sensor specific variations in sources, lens chromatic aberrations, variations in optical filters, detector heterogeneities, and other things, the relationship between absorptance and density is not theoretically predictable but has to be empirically determined for every individual sensor. Following Fratini et al. (2014), every instrument has its own factory derived calibration function (F) to describe the exact relationship between absorptance (a) and density (ρ), depending on air pressure (Pa):

$$\rho = PF(\frac{a}{Pa}) \tag{1}$$

Lens contamination due to mineral dust in the optical path more strongly affects smaller wavelengths, leading to an underestimation of ρ_c and an overestimation of ρ_v. These drift errors are usually not accounted for under the assumption, that a

Table 1. Flux data processing procedure using EddyPro software (v. 7.0.4, LI-COR Inc.).

Despiking following Vickers and Mahrt (1997) with the following plausibility ranges: W = 5.0 σ, CO_2 = 3.5 σ, H_2O = 3.5 σ, sonic temperature = 3.5 σ
Amplitude resolution: Range of variation = 3.5 σ, number of bins = 100, accepted empty bins = 70 %
Drop-outs: extreme bins = 10 percentile, accepted central drop-outs = 10 %, accepted extreme drop-outs = 6 %
Discontinuities with the following hard flags (hf) and soft flags (sf): U: hf = 4.0, sf = 2.7; W: hf = 2.0, sf = 1.3; Ts: hf = 4.0, sf = 2.7; CO_2: hf = 40.0, sf = 27.0; H_2O: hf = 40.0, sf = 30.0; variances: hf = 3.0, sf = 2.0
Skewness and **kurtosis** with the following hf and sf: Skw limits: hf = $\pm$ 2.0, sf = $\pm$ 1.0; kur lower limits: hf = 1.0, sf = 2.0; kur upper limits: hf = 8.0, sf = 5.0
Steadiness of horizontal wind: Accepted wind relative instationarity = 0.5
Axis rotation: Planar fit using 3 wind sectors (~~0~~80° - ~~80~~240°, ~~80~~240° - ~~230~~ 320 °, ~~230~~320° - ~~360~~ 80 °)
Detrending method: Block averaging
Time lags optimization: Covariance maximization with default $\pm$ 1 s
Correction for **air density fluctuations**: Application of WPL terms to fluxes (Webb et al., 1980)
Spectral corrections: Analytic high-pass filtering (Moncrieff et al., 2005) and analytic low-pass filtering (Moncrieff et al., 1997)

slow drift in mean gas concentrations (i.e. over several weeks to months) does not affect the estimation of turbulent fluctuations and, hence, of covariances. This is however not the case. In fact, Serrano-Ortiz et al. (2008) estimated, that a drift in concentration measurements will propagate into an overestimation of the carbon dioxide uptake via the WPL correction. They also showed, that this error is not evenly distributed but has a greater ~~affect~~ effect during daytime and summer, when sensible heat fluxes are large. Fratini et al. (2014) have shown, that errors in mean concentrations leak into errors in fluxes on account of amplified or dampened estimated fluctuations. Fratini et al. (2014) have also shown that both these effects can be eliminated, possibly completely, when the drift in gas concentration is corrected before raw data processing. Therefore, the offset between measured and reference (i.e. "real") gas concentrations has to be quantified and converted into the corresponding zero offset absorptance biases. Fratini et al. (2014) estimated the reference gas concentrations through linear interpolation of the zero absorptance offset between individual calibration dates, thereby assuming a constant increase of the bias. Due to the remote location on the Tibetan Plateau, user calibrations of the sensor were not performed with due regularity, making this approach not feasible in our case. Instead, we used the ~~daily mean~~ CO_2 mixing ~~ratios from the Mauna Loa atmospheric observatory (years 2005-2018, NOAA ESRL Global Monitoring Division) to fit a sine-cosine model , which was then used to determine the offset of our measurements. We~~ ratio measurements from Mt. Waliguan atmospheric observatory

(years 2005-2018, Dlugokencky et al., 2020), situated approximately 1100 km NE of Nam Co, still on the Tibetan Plateau. We averaged the weekly flask measurements to monthly means and fitted the following model to the data:

$$CO_{2\ ref}(t) = p_1 + p_2 * t + p_3 * cos(2 * \pi * t/365) + p_4 * sin(2 * \pi * t/365) + p_5 * cos(4 * \pi * t/365) + p_6 * sin(4 * \pi * t/365), \quad (2)$$

where t is the decimal time in days and p_i are the fit parameters. This model was used ~~the differences~~ to generate the 30-minute CO_2 concentration reference time series. The rationale for using this model rather than a linear or spline interpolation was to mimic the general pattern of the atmospheric CO_2 background concentration while excluding short term CO_2 variations which most likely do not affect the Mt. Waliguan observatory and our site at the same time. We then calculated the CO_2 offset used for the drift correction on a daily basis, as the difference between the daily ~~median~~ medians of the measured CO_2 ~~concentrations and the model, which was then repeated 48 times, yielding a single value for every 30-min interval. Using a sine-cosine model preserves the naturally occurring annual fluctuations in CO_2 concentrations better than, e. g. a linear model would do. The offset in~~ concentration and the reference CO_2 concentration. Hence, one offset value was applied to all 30-minute CO_2 concentration measurements of each individual day. In contrast, the H_2O ~~mixing ratios was determined using~~ offset was determined as the difference between the 30-minute H_2O concentration measured by the Li-7500 gas analyzer and the H_2O concentration calculated from auxiliary low frequency measurements of relative humidity, temperature and air pressure. ~~We~~ The time series of 30 minute concentration offset values were imported as dynamic metadata file in EddyPro. Together with the sensor specific calibration information we can use Eq. (3) (which is Eq. (10) from Fratini et al., 2014) to calculate the true absorptance (a) from measured absorptance (a_m) and any absorptance offset (a_0), which is then converted back to densities or mixing ratios.

$$a = \frac{a_m - a_0}{1 - a_0} \quad (3)$$

The ~~time series of absorptance offset values were imported as dynamic metadata file in EddyPro. It is used together with the sensor specific calibration information~~ corrected 10 Hz concentration measurements are then used to repeat raw data calculation of the fluxes and subsequent corrections, including application of WPL terms following the methodology in Sect. 2.2. Note that all conversions between absorptance and number density require the calibration function of the specific instrument.

2.4 Quality filtering

The correct application of the eddy covariance method requires a wide range of assumptions and works only within certain conditions. To ensure meaningful flux calculations, the raw data needs to be tested and flagged very thoroughly. We used the quality flags and tests implemented in EddyPro and applied additional filtering for low frequency outliers using openeddy R package from Ladislav Šigut, who implemented the quality control procedure following Mauder et al. (2013). The flagging scheme remains the same as above with "0" for high quality fluxes, "1" for intermediate quality fluxes and "2" for poor quality fluxes. As a first step, we manually removed periods with obvious sensor malfunctioning, especially in 2012 and 2018. To identify periods with insufficient turbulent mixing, we estimated the friction velocity (u*) threshold using the REddyProc R package. Fluxes with u* < 0.08 m s^{-1} were excluded from subsequent calculations. During the long measuring period, spanning

nearly 15 years, several buildings and scientific infrastructure were constructed in close vicinity of the eddy covariance tower. During the development of the NAMORS, from the foundation with only a few tents in 2005 to a well-equipped research station in 2019, we approximated five times with significant changes in constructions. In 2009 the PBL container, the shed and the solar panel were set up. In 2010 the main building and the green house were constructed. In 2012 the shed was rotated to become the laboratory and the tool shed next to the greenhouse was added. Finally, in 2019 the garage was relocated and extended south of the laboratory and the solar panels were removed. To assess possible influences on the flow and turbulence regime, we analyzed the wind direction distribution of the mean wind speed and the turbulent kinetic energy. We accounted for possibly disturbed turbulence, by applying the planar fit axis rotation for three different wind sectors during flux calculation (see Sect. 2.2). Furthermore, we generated a quality flag (qc_wind_dir) indicating whether a flux originates from a disturbed sector. Table 2 shows the disturbed sectors which were excluded from subsequent calculations. The CO_2 and H_2O fluxes and their respective densities were ~~additionally~~ checked for repeating values as they are a sign of malfunctioning equipment. We furthermore extracted hard flags of skewness and kurtosis ~~and of discontinuities~~ (see Table 1) and combined all flags to a preliminary composite which was used as a prerequisite for subsequent low frequency despiking of the flux time series. ~~To~~ Please note that the H_2O gas densities and concentrations in the EddyPro full output file are calculated mainly from low frequency measurements of air temperature, pressure and relative humidity, probably because these are deemed more accurate than the high frequency measurements of the IRGA. To enhance comparability we extracted the high frequency H_2O gas densities from the EddyPro statistics output file (variable 'mean(h2o)') and calculated the mole fraction and mixing ratio. These variables were quality filtered following the same scheme as above and are supplied with the data set (suffix: _Li7500). To account for seasonal variations, despiking is done within blocks of 13 consecutive days by comparing each record (v_i) with its neighbors via double differencing to produce its score x:

$$x = (v_i - v_{i-1}) - (v_{i+1} - v_i) \tag{4}$$

A measurement gets flagged if x is larger or smaller than the median of the scores (M_x) $\pm$ the scaled absolute median *MAD*:

$$M_x + \frac{z * MAD}{0.6745} < x < M_x - \frac{z * MAD}{0.6745} \tag{5}$$

with MAD being defined as:

$$MAD = median(x - M_x) \tag{6}$$

The constant 0.6745 in Eq. (5) corresponds to the Gaussian distribution and allows for comparability of MAD with the scaling factor z, which determines how rigorous the algorithm screens for outliers (Papale et al., 2006). The lower the value, the stricter the screening, with our setting left to the default $z = 7$. This procedure was repeated iteratively 10 times or until no outliers were detected anymore. For every measurement, the flags were combined to an overall quality flag and fluxes and concentrations with poor quality (flag = "2") were removed from subsequent computations. The quality flagged high frequency molar densities were also incorporated in the composite flag of the CO_2 and H_2O fluxes. The R script with the exact calculations can be found in the supplementary material.

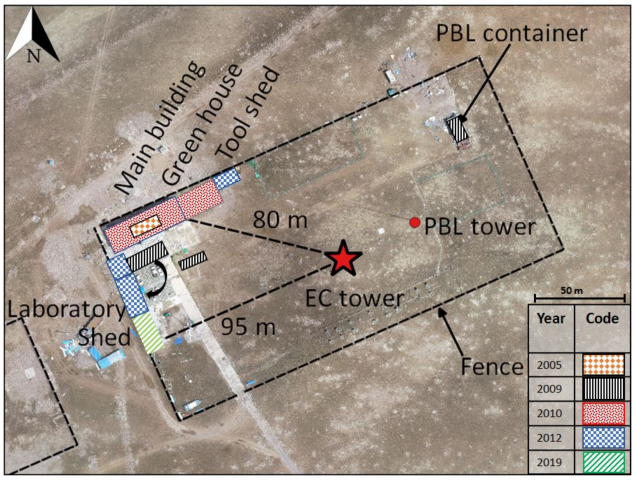

Figure 2. Map of the NAMORS station showing the identified changes in construction from 2005 to 2019. Aerial images provided by Guoshuai Zhang.

2.5 ~~Wind field analysis~~

~~In order to conduct meaningful estimations of the fluxes, the area "seen" by the measurement should represent the ecosystem of interest and the flow regime should be as undisturbed as possible (Aubinet et al., 2012). During the long measuring period, spanning nearly 15 years, several buildings and scientific infrastructure were constructed in close vicinity of the eddy covariance tower. During the development of the NAMORS, from the foundation with only a few tents in 2005 to a well-equipped research station in 2019, we approximated five times with significant changes in constructions (2). In 2009 the PBL container, the shed and the solar panel were set up. In 2010 the main building and the green house were constructed. In 2012 the shed was rotated to become the laboratory and the tool shed next to the greenhouse was added. Finally, in 2019 the garage was relocated and extended south of the laboratory and the solar panels were removed. To account for possibly disturbed turbulence, we applied the planar fit axis rotation for three different wind sectors during flux calculation (see Sect. 2.2). To assess possible influences on the flow and turbulence regime, we analyzed the wind direction distribution of the mean wind speed and the turbulent kinetic energy. Furthermore, we estimated the source area of the flux measurements by calculating cumulative footprints using the model of Kormann and Meixner (2001). This footprint model was developed for non-neutral atmospheric conditions, therefore all measurements were checked for the stability parameter $(z-d)/L \neq 0$. The model relates a flux to a certain direction in a certain distance around the EC station, depending on the measurement height, wind direction and wind speed, friction velocity, atmospheric stability and the cross stream wind component. The cummulative footprints (Fig. **??**) were calculated and plotted using FREddyPro R package. However, EddyPro also allows for the computation of flux footprints using Kormann and Meixner (2001) but supplies only the distances of flux contributions (~~

Table 2. Disturbed wind sectors and times.

From	To	Back of CSAT3	PBL container	Main buildings
2005-12-04	2009-06-30	305°–325°	-	260°–280°
2009-06-30	2010-01-30	10°–30°	30°–50°	260°–280°
2010-01-30	2011-12-31	10°–30°	30°–50°	250°–300°
2012-01-01	2018-12-31	10°–30°	30°–50°	250°–315°
2019-01-01	2019-09-07	10°–30°	30°–50°	245°–315°

2.5 Sensor self heating correction

When using an open path IRGA, it is necessary to correct for air density fluctuations caused by fluctuations of temperature and water vapor in the measurement path. The WPL correction compensates for the naturally occurring density fluctuations and should be applied in any case (Webb et al., 1980). Furthermore, especially during cold conditions (low temperatures below -10 °C), an apparent CO_2 uptake may be measured, which is caused by conductive, convective, and radiative heat exchange processes happening in the measurement path (Burba et al., 2008). These stem from heating of internal electronics during normal operation, as well as solar radiation encountered by different instrument parts surrounding the open sampling path of the sensor. This correction is necessary for pre-2010 models of the Li-7500 or for newer instruments (e.g. Li-7500A, Li-7500RS) with summer setting but used in a very cold environment (Oechel et al., 2014). Although the size of the heating correction is quite small (i.e. 10-50 times smaller than the WPL-correction) the small bias can lead to an overestimation of net ecosystem CO_2 uptake when integrating over long periods in cold environments (Oechel et al., 2014). Burba et al. (2008) developed a correction procedure which is well tested and fully implemented in the EddyPro software. The procedure depends on a range of correction factors, which were developed from the original sensor setup in Nebraska, USA. Our study site on the Tibetan Plateau displays different environmental conditions than those in which the correction was tested, namely an inclined IRGA, lower ambient temperatures and strong winds, as well as possible snow and ice deposits on parts of the instrument. ~~No independent gas concentration measurements are available from our study site which could be used for fine tuning of the air density correction. Hence, we applied the approach by Oechel et al. (2014), who developed an empirical method to calibrate the correction of EC measurements, originally for a sensor in Alaska. We made the same assumptions as Oechel et al. (2014) concerning the relationship between the vertically aligned sensor Burba et al. (2008) used in the original method in Nebraska in comparison to our aligned sensor in Tibet: The sensor consists of a bottom, cylinder-shaped part and a top, ball-shaped part which are differently exposed to ambient conditions (e.g. solar radiation) depending on the inclination of the sensor. While the top, ball-shaped part of the sensor is about equally exposed in Nebraska and Tibet, we assume the inclined bottom cylinder in Tibet to be more exposed to radiation than the vertical aligned bottom cylinder in Nebraska. Its temperature (T_{botTI}) is a combination~~ In a recent publication, Frank and Massman (2020) tested the correction procedure for a "cold, windy, high-elevation mountainous site" and found inconsistencies in the Burba et al. (2008) correction: (1) The

Burba et al. (2008) correction contains boundary layer adjustment terms for non-flat surfaces but the top- and bottom surfaces of the Li-7500 are flat. This leads to an underestimation of the surface heat fluxes which is an order of magnitude too small. (2) The weightings of the bottom ~~cylinder temperature in Nebraska (T_{botNE}) and the top ball temperature in Nebraska (T_{topNE}) adjusted with a weighting factor x.~~

$$T_{botTI} = xT_{botNE} + (1-x)T_{topNE}$$

~~The weighting factor x has to be parameterized by calculating the sensor self heating correction using Method 4 (submethod: linear regression with air temperature Burba et al., 2008) for multiple weighting factors. The optimal weighting factor is selected on the basis of two criteria: First, periods have to be identified when a change in CO_2 efflux with temperature can be assumed to be negligible. For our study site on the Tibetan Plateau, we assume negligible CO_2 efflux when air temperature is below -15 °C and soil moisture below 2 % during the months of January and February. The ground can be regarded as continuously frozen since two months, with mean air temperatures below 0 °C at least since November. By then, freezing should have pushed any excess CO_2 out of the soil. During these cold conditions, the flux-to-air temperature slope was calculated for every weighting factor (0-100). The CO_2 fluxes should not change with temperature during these cold conditions, hence the closer the slope to zero,~~ and top surface heat fluxes are "improbable and an order of magnitude too large" (Frank and Massman, 2020). While these errors canceled out during the study of Frank and Massman (2020), this may not be the case for other field sites. Following the recommendations of Frank and Massman (2020), we discarded the boundary layer adjustment terms for non-flat surfaces from the calculations and applied their newly calculated weightings of the bottom and top surface heat fluxes, thus emphasizing the role of the ~~better. Second, the direction of the corrections for every weighting factor was examined for periods where a negative correction would be implausible. Because the electronics of the pre-2010 model of the Li-7500 are kept at about +30 °C, the sensor should on average be warmer than the ambient air. A negative daily correction would implicate, that the ambient air is warmer than the sensor surface which is implausible at temperatures below 0 °C. Hence, the number of negative daily corrections at air temperatures below 0 °C should be small, which is the second criterion to find the optimal weighting factor. The optimal weighting factor is then used to correct all measurements when ambient temperature is below 0 °C. We used a radiation threshold of 5 W m^{-2} to distinguish between daytime and nighttime. The method is described in detail in Oechel et al. (2014) and the R script with the exact calculations can be found in the supplementary material~~spar in self heating. We first reproduced the Burba et al. (2008) correction like it is implemented in EddyPro and then adjusted the equations as described above. Please note that we used the quality filtered variable co2_molar_density from the EddyPro full output file in order to reproduce the calculations.

2.6 Gap filling

In order to obtain a CO_2 flux time series as complete as possible, we filled the data gaps using the marginal distribution sampling (MDS) algorithm (Falge et al., 2001; Reichstein et al., 2005), implemented in the REddyProc R package by Wutzler et al. (2018). Depending on the length of the data gap and the availability of the meteorological input variables radiation (Rg), air temperature (Tair) and water vapor deficit (VPD), the missing CO_2 flux values are derived from a look up table (LUT)

or from mean diurnal course (MDC). The LUT approach replaces the missing value with the average value under similar meteorological conditions within a certain time window. Meteorological conditions are similar if Rg deviates not further than 50 W m^{-2}, Tair not further than 2.5 °C and VPD not further than 5.0 hPa. If no similar conditions can be found within an appropriate time window, the missing value is replaced using the average value at the same time of the day (1 hour) (MDC). If the missing value can not be filled during the initial time period (7 - 14 days), the time window size is increased and the procedure repeated until the value can be filled or the data gap gets too long for reliable gap filling (i.e. > 60 days). ~~As horizontal wind speeds are generally very high (lowest percentile = 0.47 m s^{-1}) at our study site, we did not filter for low friction velocity. The full MDS algorithm is described in Wutzler et al. (2018) and the R script used in this study can be found in the appendix.~~

Prior to the processing, we excluded the lower and upper 0.2 % of the fluxes and discarded physiological implausible night time fluxes < -0.1 µmol m^{-2} s^{-1}. To estimate the uncertainty of the ~~gap-filling~~ gap filling procedure, we used the method implemented in REddyProc R package, which, besides filling real gaps, creates artificial gaps from otherwise available data and fills them in the same way as if it was a real gap (see section 2.6). The model-value residual should be considered when aggregating the gap-filled time series to daily or annual estimates of NEE, GPP and R_{eco}. We included the filled values for the artificially created data gaps, as well as quality flags for the gap filling procedure, with "0" for measured data, "1" for high reliability, "2" for intermediate reliability and "3" for poor reliability of the gap-filled values. The full MDS algorithm is described in Wutzler et al. (2018) and the R script used in this study can be found in the appendix.

2.7 Flux uncertainty estimation

As with all measurements, the reported fluxes are subject to uncertainty, consisting of a systematic and a random part. Systematic uncertainties may occur e.g. from having an imperfect measurement setup or, like in our case, due to limited maintenance and calibration of the sensors (see section 2.3). We applied a wide range of methods to filter and compensate for systematic errors. Most importantly, we tested for fulfillment of basic EC assumptions using integral turbulence characteristics and steady state test (e.g., Foken and Wichura, 1996) and compensated for air density fluctuations and high- and low-frequency losses (see Sect. 2.2, 2.4 and 2.5). In contrast to systematic uncertainties, random errors do not bias the flux in any direction but reduce the overall confidence (i.e. precision) of the reported values (Richardson et al., 2012). Random uncertainties mainly arise from the stochastic nature of turbulence, footprint variability, as well as from instrument noise and the resolution at which samples are recorded (Richardson et al., 2012). Hence, it is important to estimate the random uncertainty, especially in places with rather low magnitude of fluxes, as it is in our case. We estimated the random flux error (RE) using the mathematically rigorous and fully implemented approach by Finkelstein and Sims (2001). This method calculates the ~~random flux errors~~ uncertainty arising from insufficient sampling of large eddies with high spectral energy, the so-called sampling error. As these large turbulences appear irregularly during sampling, the error is random and can be estimated. First, the so-called Integral Turbulence time-Scale (ITS) is calculated. Basically, the ITS is the covariance between vertical wind velocity and gas concentration as a function of lag time between these two time series (Holl et al., 2019). With increasing time lag, the cross correlation function typically decreases towards values close to zero, indicating an increasing non-correlation of the two time series. In practice, the correlation function must be stopped, otherwise it would go infinitely towards zero. We stopped the integral as soon as the

cross-correlation function (~~–~~ which always starts at 1 ~~)~~ crosses the x-axis (i.e. first crossing 0). In case the cross-correlation function would never cross the x axis, a default time value can be provided at which the function is stopped. We set this "maximum correlation period" to 5 s in order to keep computational performance high. Once the ITS is calculated, the ~~random uncertainty of the fluxes~~ RE can be estimated based on the calculation of the "variance of covariance" (Finkelstein and Sims, 2001).

~~It is important to note, that the random error estimate applies to the uncorrected fluxes, i.e. before correction for spectral attenuation and air density fluctuations. In order to estimate the random error of the finally corrected fluxes, the propagation of error through the corrections has to be taken into account, especially for the estimation of long-term NEE (Liu et al., 2006) .First, we multiplied the errors with the same spectral scaling factor as the fluxes to account for spectral attenuation. Then, we used Eq. (1) and (2) from Burba et al. (2008) to apply the WPL correction to the flux errors. Following basic concepts of error propagation, we corrected the random uncertainties the same way as if they were fluxes but adding them up in rooted quadrature using Eq. (**??**) for random error of water vapor flux and Eq. (**??**) for random error of CO_2 flux.~~

~~$$RE_E = (1+\mu\sigma)\sqrt{{RE_{E_0}}^2 + (\frac{RE_H}{\rho C_p}\frac{\rho_c}{T_a})^2}$$~~

~~$$RE_{F_C} = \sqrt{{RE_{F_{C0}}}^2 + (\mu\frac{RE_E}{\rho_d}\frac{\rho_c}{1+\mu\sigma})^2 + (\frac{RE_H}{\rho C_p}\frac{\rho_c}{T_a})^2}$$~~

~~RE_E and RE_{F_C} are the WPL-corrected water vapor and CO_2 flux errors (kg m^{-2} s^{-1}) . RE_{E_0} and $RE_{F_{C0}}$ are the initial water vapor and CO_2 flux errors (kg m^{-2} s^{-1}), not corrected for WPL, but already multiplied by the spectral correction factors. RE_H is the sensible heat flux error, already corrected for WPL and spectral correction factor (W m^{-2}). μ is the ratio of molar masses of air to water ($\mu = 1.6077$), σ is the ratio of the mean water vapor density (ρ_v in kg m^{-2} s^{-1}) to mean dry air density (ρ_d in kg m^{-2} s^{-1}) . ρ_c is the mean ambient CO_2 density (kg m^{-2} s^{-1}) and ρ is the mean total air mass density (kg m^{-2} s^{-1}) . C_p is the air heat capacity (J kg^{-1} K^{-1}). The a posteriori sensor self heating correction (Sect. 2.5) does not include other scalars with quantified random error within its equations. Hence, the propagated random CO_2 flux error remains the same before and after self heating correction.~~ Because the RE method is based on the half hourly auto- and cross-correlation of the vertical wind component and the scalar of interest (e.g. air temperature or gas concentration), it contains only very limited information about spatial, temporal or meteorological variability (El-Madany et al., 2018). During the MDS gap filling procedure (Reichstein et al., 2005), the missing NEE values are (mostly) calculated using a look-up table approach with quite narrow meteorological bins (bin width: Rg = 5 W m^{-2}, VPD = 5 hPa, Tair = 2.5 °C) within a short time window (+/- 7 days). During these conditions, the vegetation should not change a lot and hence, the ecosystem response to atmospheric drivers should remain the same. Any variability of the flux measurements probably stems from the temporal (+/- 7 days sampling window) and spatial (changes in footprints between 30-min fluxes) heterogeneity at the site. Hence, we could use the standard deviation of the fluxes used for gap filling (NEE_fsd) as an additional measure for flux uncertainty to complement the random uncertainty estimation of Finkelstein and Sims (2001).

3 Results

3.1 Drift correction

Figure ~~?? illustrates how the drift correction works quite well.~~ 3 illustrates the effect of the drift correction: Before drift correction, the CO_2 mixing ratios were underestimated substantially. Note the rapid divergence from the model after user calibrations were performed in 2009, 2012 and 2019. In June 2017 the original sensor was replaced with another one that was factory calibrated in March 2016. The drift correction eliminates the daily divergence from the modeled background concentration while keeping high frequency fluctuations for computation of the 30-min averaged fluxes. Remember that the drift correction applies an offset to the raw data and is subject to the subsequent flux calculation and correction procedures. Before application of WPL and spectral attenuation terms, the corrected fluxes yielded higher carbon uptake during daytime and summer, than the uncorrected fluxes. If the WPL and spectral attenuation correction is taken into account, the carbon uptake of the drift corrected fluxes gets considerably smaller than the uncorrected fluxes, especially during times with high sensible heat fluxes~~(see Fig. 8).~~ . The findings are in compliance with instrument theory of operation and the results from numerical simulations and field data analysis as conducted by Fratini et al. (2014) and with Serrano-Ortiz et al. (2008), who analyzed the propagation of a systematical underestimation of the CO_2 concentration on the CO_2 fluxes via the WPL terms. However, the software implementation of the drift correction is still in development and was not yet officially released (i.e. you can not use it via the GUI), so unfortunately it still contains a software error (bug): Every data gap in the H_2O reference concentration time series (due to e.g. missing low frequency meteorological data) produces a corrupted H_2O mixing ratio record in the following half hour, which also affects the calculation of the CO_2 mixing ratio. This issue was raised with the EddyPro developers and will be fixed in one of the upcoming releases. Because this error does not affect the calculation of the fluxes or other variables, we removed the erroneous values by setting plausibility limits.

3.2 Data availability and quality filtering

Table A1 lists the ~~overall~~ yearly CO_2 and H_2O flux data availability after raw data processing ~~, QC filtering and despiking, relative to the respective year.~~ and application of the various quality flags (wind direction, Ustar and QC, including flux despiking). After raw data processing, more than 50 % of the CO_2 fluxes are available for the years 2007 to 2011, as well as for 2017. Two periods with obviously corrupted flux measurements were excluded from the data set right after raw data processing. CO_2 and H_2O fluxes and concentrations were discarded from 2012-01-30 02:00 to 2012-08-31 15:00 and from 2018-06-01 00:00 to 2018-06-30 23:30 due to sensor malfunctioning. All times are in China Standard Time (CST, UTC+8), which is approximately 2 hours later than local solar time. Figure 5 shows the data availability of the CO_2 fluxes throughout the individual years before and after gap filling (see also Sect. 2.6). The overall data availability differs substantially between the years. In 2013 more than 90 % of the data are missing. In 2014 the complete winter period is missing and about one year of data is missing from May 2018 to May 2019. Continuous data gaps of up to six months occur irregularly throughout the whole data set, whereas shorter gaps can be found within periods of continuously available data. The large gaps occurred mainly due to hardware errors and power ~~shortages~~ outages whereas smaller gaps are caused by raw data processing and subsequent

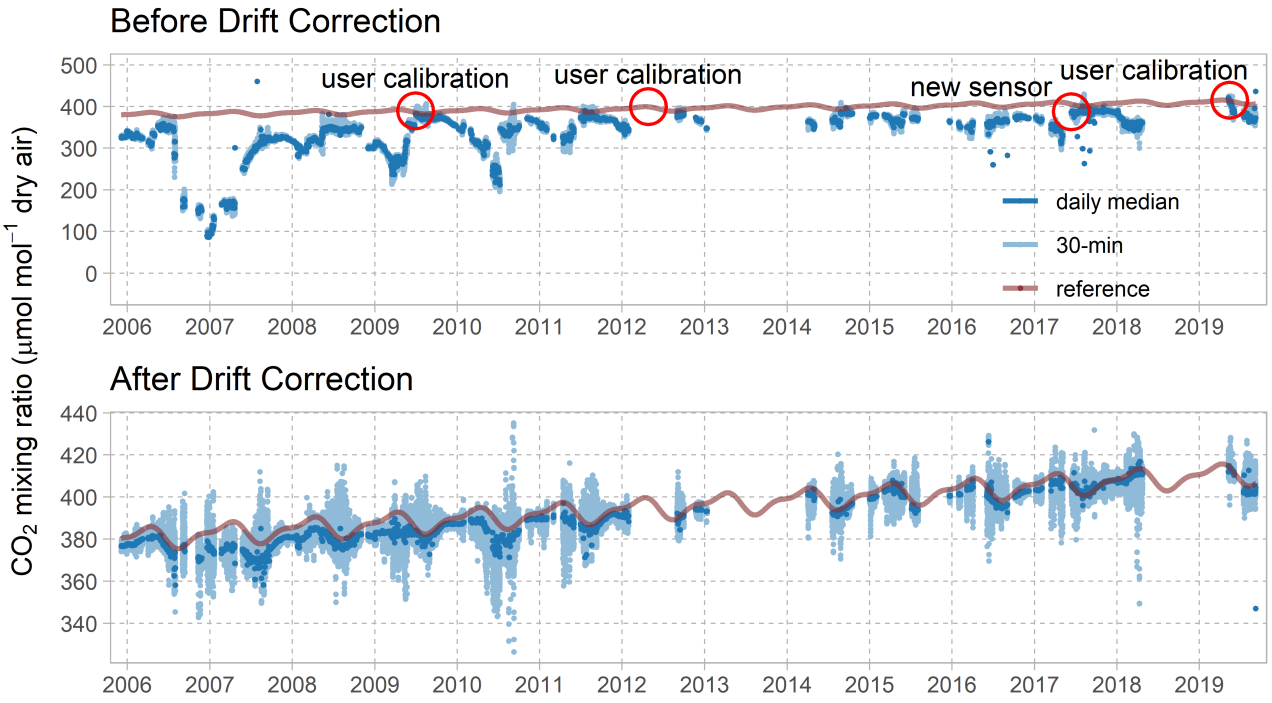

Figure 3. Daily median and 30-min CO_2 dry air mixing ratios and modeled CO_2 background concentration before and after drift correction. CO_2 mixing ratios have been checked for repeating values and outliers using the same algorithms as in Sect. 2.4. Please note the different y-axis scales.

filtering of fluxes with poor quality or due to violation of basic EC assumptions (see Sect. 2.2 and 2.4). ~~Two periods with obviously corrupted flux measurements were excluded from the data set right after raw data processing. CO_2 and H_2O fluxes and concentrations were discarded from 2012-01-30 02:00 to 2012-08-31 15:00 and from 2018-06-01 00:00 to 2018-06-30 23:30 due to sensor malfunctioning. All times are in China Standard Time (CST, UTC+8). For the years 2007 to 2011, as well as for 2017, more than 50 % of the CO_2 fluxes are available.~~ NEE gap filling increased the overall data availability for CO_2 fluxes from ~~48.3 % to 66.2~~ 52 % to 72 % in total, with seven complete years. The data set contains quality flags for each flux, indicating whether it was gap filled and how well the gap filling mechanism performed (Reichstein et al., 2005). The quality of the gap filled fluxes was derived by treating individual available values as data gaps and filling them as if they were real data gaps. When aggregating the residuals to an overall error estimate of the model performance, autocorrelation has to be taken into account because no independent training data is available. The model-data residuals were checked for empirical autocorrelation, indicated positive autocorrelation until a lag of up to 65 records, decreasing the number of effective observations from ~~70758 to 8712.~~ 62465 to 7047. Taking this into account, Pearsons correlation coefficient is ~~0.83~~ 0.91 with a root mean square error (RMSE) of ~~2.6~~ 1.6 µmol m^{-2} s^{-1}.

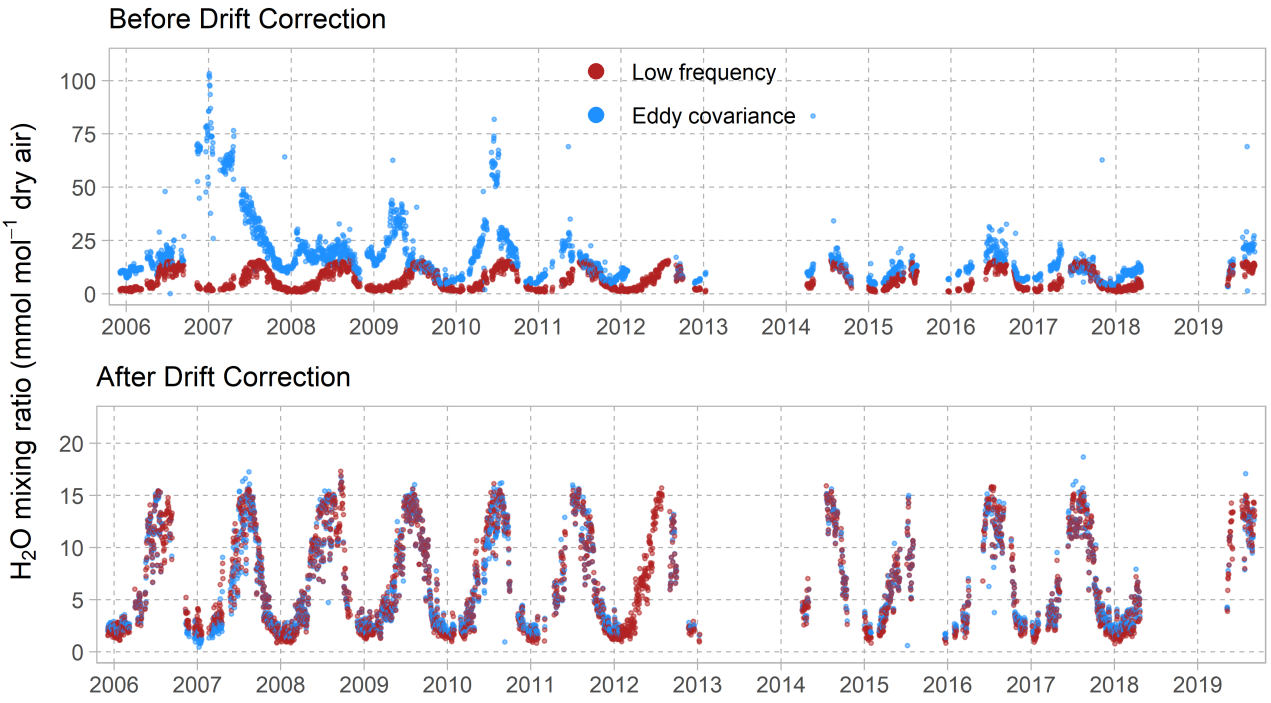

Figure 4. Half hourly H_2O dry air mixing ratios and low frequency reference concentration before and after drift correction. H_2O mixing ratios have been checked for repeating values and outliers using the same algorithms as in Sect. 2.4. Please note the different y-axis scales.

3.3 ~~Wind field analysis~~

~~Cummulative flux footptints before and after the construction of the main building in 2010. The point $x = 0$ and $y = 0$ represents the position of the Eddy Covariance station. The disturbed (sealed) areas are illustrated by red polygons. Aerial images provided by Guoshuai Zhang.~~ ~~Wind roses showing the wind speed distribution and turbulent kinetic energy (TKE) in 5 ° binned wind directions at NAMORS EC station before and after 2010~~ Figure 2 shows how constructions changed in 2009, 2010, 2012 and 2019. It was not possible to assess when exactly the different buildings were constructed, hence we focused on the single most severe change, the set up of the two-storey main building in 2010. To assess the impact on the wind field, we calculated ~~cumulative flux footprints (Fig.**??**) and~~ wind rose plots for wind speed and TKE (Fig. 6) before and after 2010. It is to note that the wind regime is superimposed by large and small scale circulation systems. During summer, the Indian and East Asian summer monsoon blow from the southern directions and during winter, the westerlies provide air masses from western directions. Furthermore, the wind may be deflected along the Nyainqêntanglha range and exhibits a diurnal pattern due to a land–lake circulation system, caused by the large water masses of Nam Co (see also Biermann et al., 2014). Nevertheless, the differences before and after 2010 are clearly identifiable. A shift in the wind direction contribution away from the building and towards more western directions can be observed. Furthermore, wind speed and TKE increase substantially in western

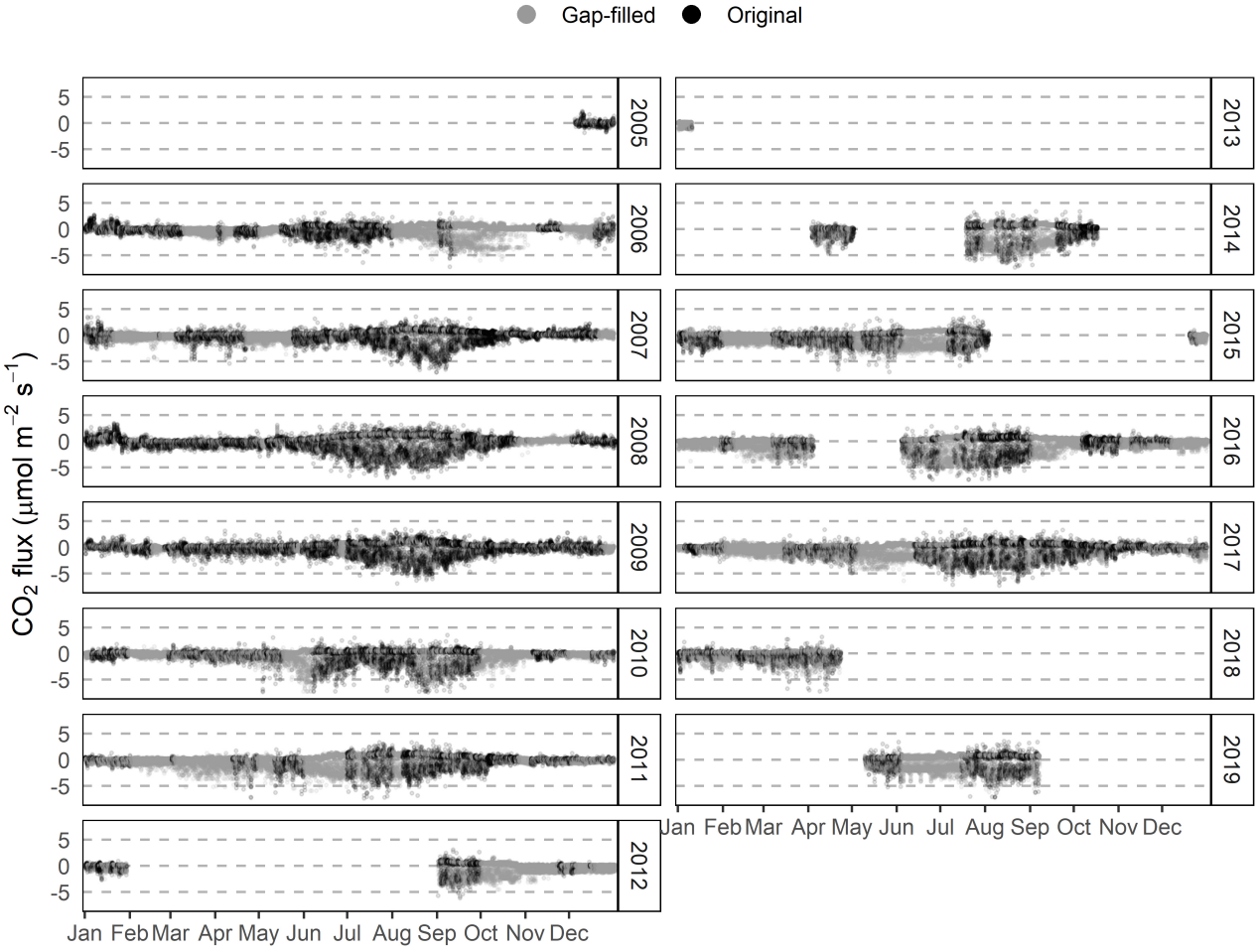

Figure 5. Data ~~Availability~~ availability after gap filling using ~~REddyProc~~MDS algorithm (Wutzler et al., 2018).~~Design modified from Holl et al. (2019).~~

direction while decreasing in the direction of the main building. ~~The cumulative footprints show complementary behavior. The main source area is a 150 m circular around the EC station, covering the buildings and sealed area, as well as the alpine steppe ecosystem within and outside the fenced area. In general, the size of the footprint gets smaller the stronger the atmosphere is mixed. The footprints at NAMORS follow this scheme, indicating an increase of the turbulent mixing in the lee of the different buildings. Fluxes $\geq$ 50 % contribution from the disturbed areas were excluded from further analyses. The ROI boundary is indicated in Fig. 2.~~

3.3 Sensor self heating correction

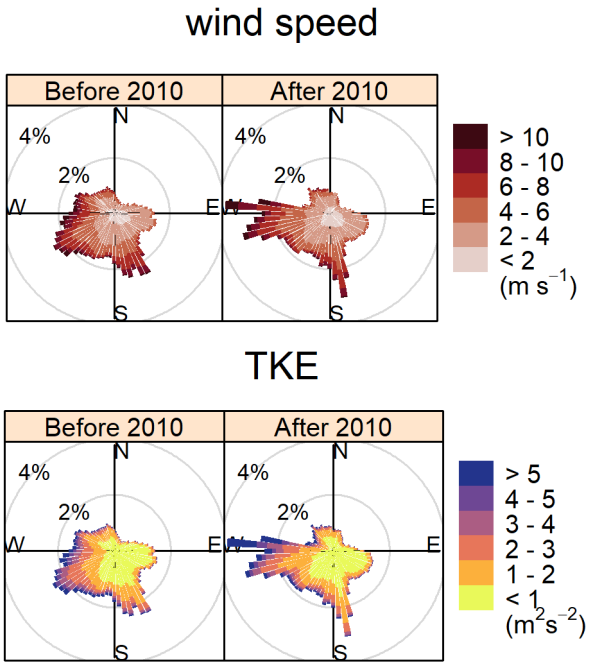

Figure 6. Wind roses showing the wind speed distribution and turbulent kinetic energy (TKE) in 5 ° binned wind directions at NAMORS EC station before and after 2010.

~~The~~ The monthly mean diurnal course of the three CO_2 flux time series in Fig. 7 clearly shows the effect of the sensor self heating correction ~~was applied~~ during cold conditions (air temperature < 0 °C)~~after it was adjusted to meet local site conditions. Following Oechel et al. (2014), the weighting factors were iteratively chosen according to the flux-to-air temperature slope closest to zero below -15 °C while keeping the smallest number of mean daily negative corrections below 0 °C. Table ?? shows the bounding conditions for the weighting factors. With 61 % to 39 % weighting, the corrected daily~~. The effect of the correction procedure following Burba et al. (2008) and the revised equations of Frank and Massman (2020) are very similar. We see various problems associated with the SSH corrections: (1) the corrections create strong artifacts during the transition between day and night, (2) SSH-corrected nighttime CO_2 fluxes ~~at temperatures below -15 °C had minimal slope with air temperature while allowing one negative daily correction at temperatures below 0 °C. Increasing the weighting factor led to steeper CO_2 flux-to-air temperature slope, which is physiologically unlikely. Decreasing the weighting factor led to a higher number of negative daily corrections which is implausible from the fundamental thermal exchange between the instrument which is controlled at +30 °C and ambient air temperatures below 0 °C. Figure 8 shows that the apparent CO_2 uptake during cold conditions was efficiently removed by the correction. The heating correction had the greatest effect during daytimewhen solar radiation additionally heats the inclined sensor. Before the correction,~~ during the cold months are very high — at about the same level as the nighttime CO_2 fluxes during summer — suggesting an over-correction of SSH effects, and (3) the winter-time

diurnal course of CO_2 flux with daytime uptake of CO_2 –- which is assumed to be the effect of the SSH -– does not disappear, but the daytime CO_2 flux is merely offset by what seems to be a more or less constant flux value. This leads us to the conclusion that the effect of the SSH is very small at our site and that the ~~fluxes were small but negative, suggesting~~ application of the standard correction (Burba et al., 2008) and its improved version Frank and Massman (2020) lead to an undue over-correction of this effect. To test our conclusion about the SSH effect at our site, we calculated the mean diurnal course of CO_2 fluxes during cold periods with a closed snow cover (Fig. A1). Under these (rare) conditions, we expect a negligible CO_2 uptake, so the SSH effect should become visible. Indeed, the not SSH-corrected CO_2 flux shows only a very small diurnal pattern with CO_2 uptake during daytime. This could still be a real physiological signal due to snow free patches in the EC footprint, or the SSH effect, or a combination of both. In any case, the daytime CO_2 uptake ~~even during very cold conditions . After the correction, the fluxes remained small but became positive , suggesting small respiration activity. Although the standard deviation of the mean daily corrections crossed the zero in almost all cases, the resulting fluxes are significantly different from zero ($p < 0.05$)while we allowed one occurrence of a negative daily heating correction.~~ under these conditions and hence the SSH effect at our site is very small. In contrast, both the SSH corrections create large positive offsets in the CO_2 flux which are clearly an overcompensation of the SSH effect.

~~The bounding conditions for the adjustment of the inclined sensor in Tibet~~

3.4 Flux uncertainty estimation

Figure 8 shows the mean diurnal and annual cycle of the CO_2 flux and the respective uncertainties. The two uncertainty estimates (RE, NEE_fsd) follow a distinct distribution, thereby reflecting the different sources of error they represent. As expected, the random uncertainty remains much lower than the standard deviation of the gap-filled fluxes (medians of 0.2 and 0.5 µmol m^{-2} s^{-1}, respectively). The RE exhibits roughly the same magnitude throughout the year whereas the NEE_fsd increases with increasing flux magnitude. Concerning the diurnal course, we see lower uncertainties during nighttime and winter than during daytime and summer. The RE is generally smaller during night while during daytime, the uncertainties almost converge.

4 Discussion

To produce an accurate and consistent time series of CO_2 fluxes, we applied several correction procedures and rigorously checked for data quality constraints during the long observation period, spanning almost 15 years. Nevertheless, some uncertainties remain, mainly due to technical and logistical constraints, as well as limited documentation of the measurements.

We applied the drift correction in order to remove a systematic bias in concentration measurements. Although the correction procedure itself works well, there are certainly other effects that could reduce the effective removal of the concentration drift. The use of the ~~Mauna Loa~~ Mt. Waliguan time series as input for the model, which was used to derive the offset between measured and "real" CO_2 concentration, may be responsible for some degree of error. First, the measurements at ~~Mauna Loa represent the northern hemisphere~~ Mt. Waliguan represent the atmospheric background CO_2 concentration 1100 km NE of Nam

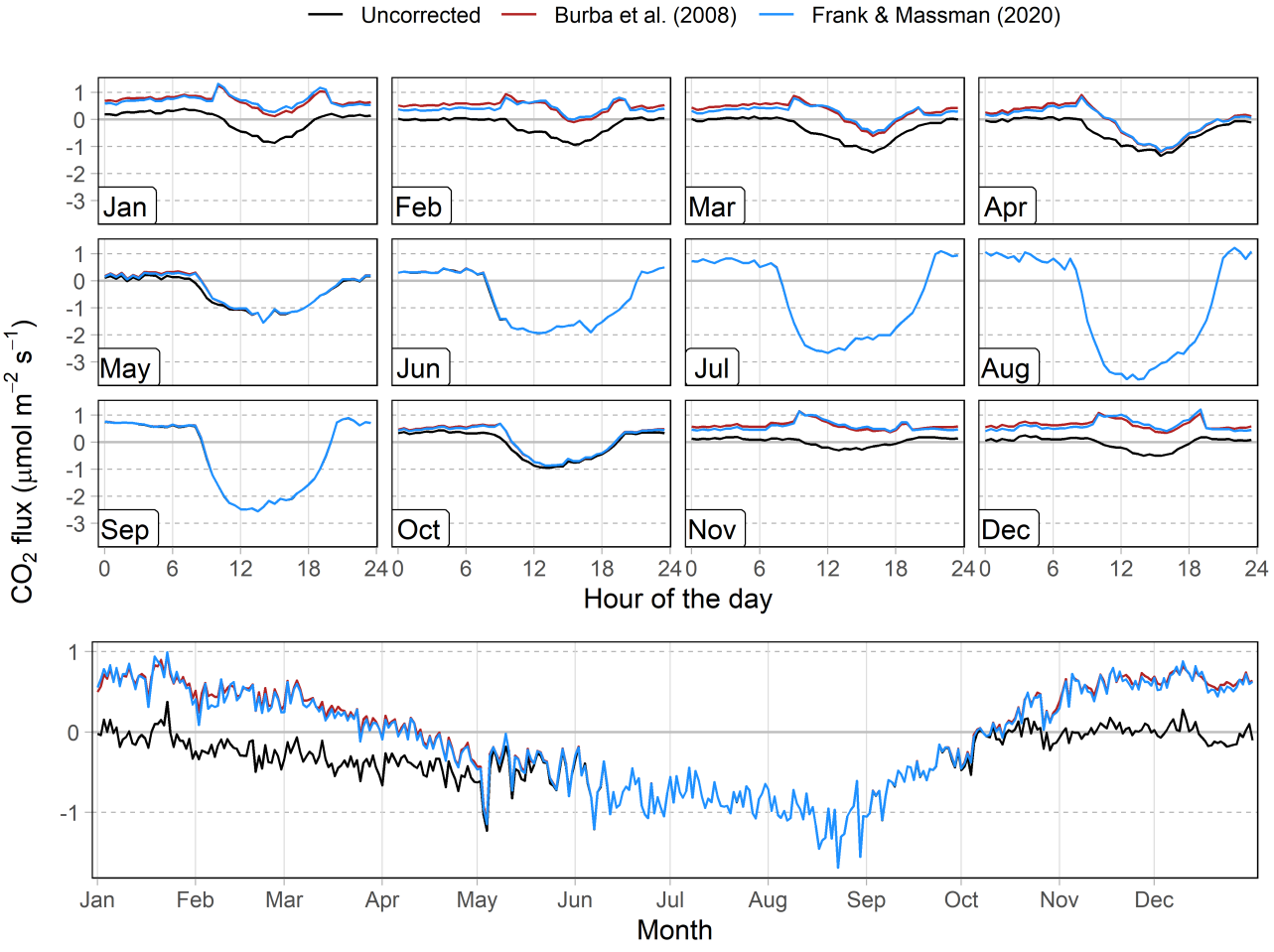

Figure 7. Monthly mean daily course and annual course of daily mean of the CO_2 flux of the years 2005 to 2019 before and after sensor self heating correction following Burba et al. (2008) and Frank and Massman (2020).

Co, which does not necessarily mean, that they also represent the CO_2 concentrations at our study site. Second, the value used to estimate the offset was derived from a model. This approach somewhat smoothes the time series and generates the same annual pattern for every year while applying a constant rise in CO_2 concentrations. There is a good agreement between the two time series when sensor calibrations have just been conducted (red circles in 2009, 2012, 2017 and 2019 in Fig. ~~??).~~ 3). To be more precise on that, the measured daily medians remain approximately 10-15 ppm lower than the model right after user calibration was performed. An underestimation of 15 ppm around 400 ppm means about 3.75 % error in concentration, which leads to roughly 1.5 % error in flux for CO_2 (the % error in flux is roughly 40 % of the % error in concentration, Fratini et al., 2014). Considering that the measured concentrations are often 100 to several 100 ppm away from the (assumed) real concentration

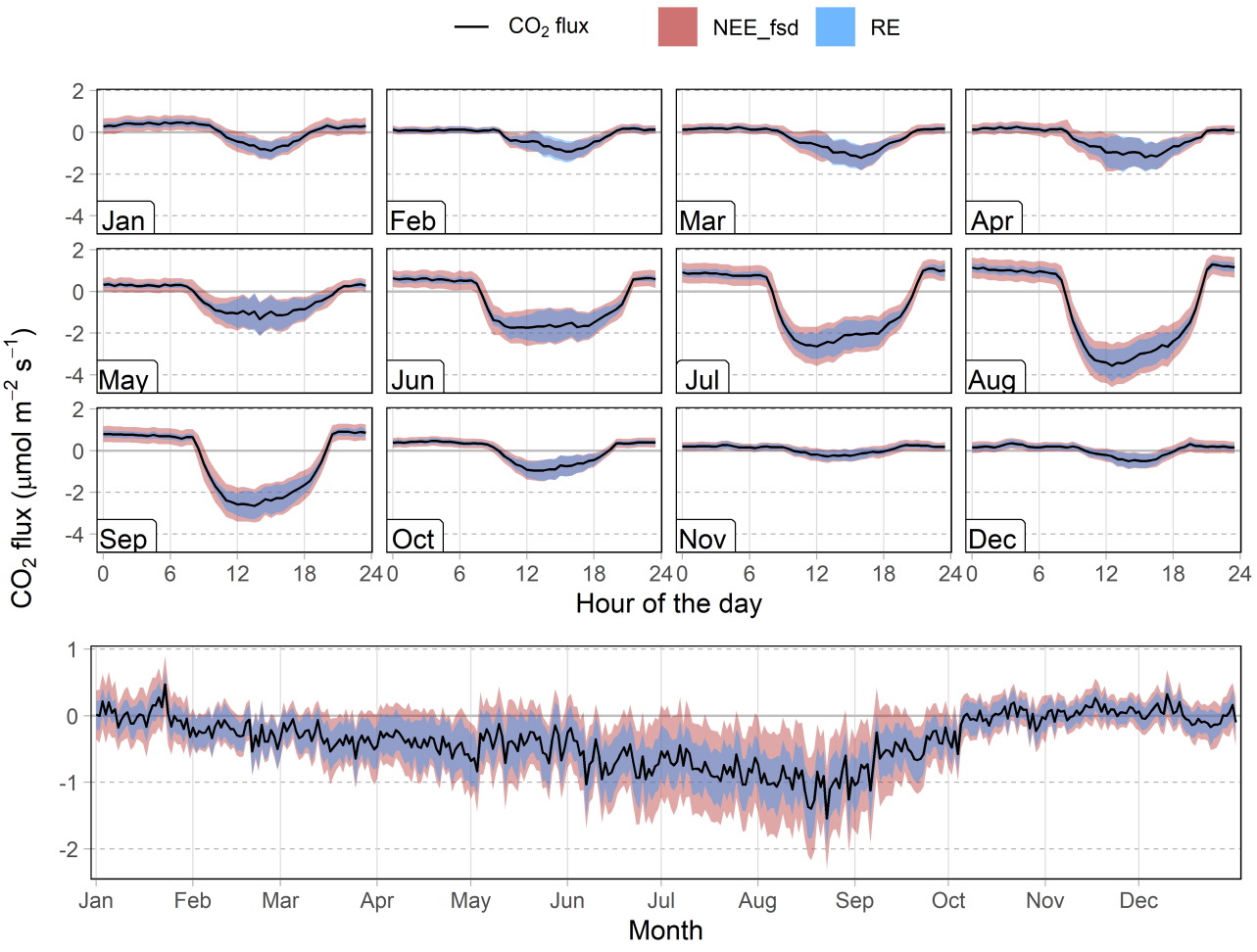

Figure 8. Monthly ~~median daily~~ mean diurnal course and annual course of daily ~~median~~ mean of the CO_2 flux and uncertainty estimates: RE is the random uncertainty ~~before and~~ following Finkelstein and Sims (2001), NEE_fsd is the standard deviation of values used for gap filling after ~~sensor self heating correction (i~~Reichstein et al. (2005).~~e. "SSH") of the years 2005 to 2019~~

and that this causes great errors in the raw flux and the WPL correction, this correction can be assumed to greatly reduce these errors. As seen in Figs. 3 and 4, after drift correction, the mean CO_2 and H_2O concentrations are very close to the (assumed) values. So even though not completely accurate, this strategy is expected to at least reduce the inaccuracy of the computed fluxes. Concerning the drift correction of the H_2O measurements, the offset was derived from adjacent low frequency
465 measurements of relative humidity, air temperature and air pressure. Although the approach itself is robust, there may be some degree of uncertainty due to the limited long term stability of the measurements which is claimed by the manufacturer ~~with~~ to be "better than 1 % RH per year" (Vaisala, 2006).

During the long observation period the surrounding of the EC system was subject to rather profound changes in constructions and scientific infrastructure. The wind regime changed substantially with the construction of the two-storey main building in 2010. The horizontal wind is forced to flow around this large obstacle, thereby increasing wind speeds and turbulent mixing reaching the EC system from western direction. Although the other constructions seem not to exhibit such a profound impact on the horizontal wind speed, some stronger turbulent mixing can be observed in the lee of the smaller buildings, such as the PBL container and the laboratory. ~~The footprints display a complementary pattern, with smaller extend in areas with increased turbulent mixing.~~ To address a possible influence by human activity, fluxes ~~with large contributions (i.e. $\geq$ 50 %) beyond the ROI~~ which originate from the disturbed sectors should be excluded from further analyses.

The use of a pre-2010 model of the Li-7500 open path IRGA usually requires the correction for apparent off-season CO_2 uptake due to air density fluctuations in the measurement path of the sensor (i.e. sensor self heating correction). We ~~calibrated the procedure to meet local site conditions using the approach by Oechel et al. (2014) that relies on the identification of conditions with negligible CO_2 efflux. For the definition of these conditions, the same concerns as already mentioned by Oechel et al. (2014) also apply to our study: While, e. g. Wang et al. (2016) found carbon exchange of Tibetan alpine steppe during winter close to zero, it is still likely that even under the coldest conditions, microbial respiration may result in a temperature-dependent small source of CO~~found the SSH effect to be rather small at our study site and moreover, the SSH corrections following Burba et al. (2008) and Frank and Massman (2020) clearly overcompensated the effects. Furthermore, we assume that there is a real daytime CO_2 uptake during winter at our study site. This could be explained by the scarce snow cover and the generally high solar radiation even during the coldest months. Measurements of surface temperature (soil temperature in 0 cm depth) show temperatures well above 0 °C during daytime in winter (mostly between 12:00 and 18:00, see Fig. A2). Plants may photosynthesize until below -3 °C, at least they do so in Antarctic tussock grass (Bate and Smith, 1983) and lichens may photosynthesize under even colder conditions (Kappen et al., 1996). In summary, we suggest that the CO_2 ~~(Panikov et al., 2006). Hence, the actual CO_2 efflux may be larger than reported here due to an underestimation of the heating correction. Furthermore, the adjustment of the inclination presented above relies on significant empiricism and a number of assumptions, which add up to the already significant assumptions made by Burba et al. (2008) for the heating correction of a vertical aligned sensor. Hence, the method still represents a site-specific approximation which should be subject to optimization and automation approaches~~uptake during winter daytime represents a physiologically meaningful signal rather than an artifact from the SSH effect. Further research should be performed to better disentangle the two effects, hence we provide the following CO_2 flux time series: (1) no SSH correction applied, (2) SSH correction following Burba et al. (2008) applied, and additionally, (3) SSH correction following Frank and Massman (2020) applied.

While systematic errors can be corrected efficiently, random errors may only be quantified in order to derive the overall precision of the measurements. Figure 8 shows the monthly ~~median daily~~ mean diurnal course of the CO_2 fluxes and their random uncertainties ~~(Finkelstein and Sims, 2001) after correction for spectral attenuation and air density fluctuations (WPL and sensor self heating~~(RE and NEE_fsd) from every available measurement throughout the long time series (without gap-filled values). ~~When using an open path IRGA to determine gas densities, errors in the measurement of fluxes do not propagate proportionally through the WPL algorithm. In fact, the~~ The magnitude of these errors depends strongly on the sensible heat flux (Liu et al.,

2006). Hence, the random flux errors are especially pronounced during daytime and summer, when sensible heat fluxes are large. During winter (November to February), the random error oftentimes exceeds the magnitude of the fluxes. The random uncertainty ~~estimate described above represents a conservative value, as it specifically addresses the turbulence sampling error~~ estimates described above represent random flux components as well as spatial heterogeneity, temporal variability, and small meteorological variability while neglecting other sources of random flux errors such as instrument noise~~and footprint variability~~.

One uncertainty, about the type of alpine steppe that the fluxes are supposed to represent, still exists. The whole NAMORS station was fenced in 2006, thus preventing the otherwise ubiquitous livestock from grazing in the footprint area. Wei et al. (2012) carried out chamber measurements within and outside the fenced area at the Nam Co station during the growing seasons of 2009 and 2010. The period of 4 years of livestock exclosure significantly increased above ground biomass which possibly led to lower soil temperatures due to shading effects. While the authors did not find a significant effect on CO_2 emission patterns during the two growing seasons, CO_2 emissions tended to be less sensitive to temperature change (i.e. lower Q_{10} value). Their findings are corroborated by Hafner et al. (2012) who used ^{13}C pulse labeling to assess the carbon cycle of a montane *Kobresia* pasture with moderate grazing and a 7-year-old grazing exclosure plot in the province of Qinghai on the north-eastern TP. While the total CO_2 efflux of the grazed and ungrazed grasslands remained similar, the grazing exclosure had a negative effect on organic carbon stocks in the upper 15 cm of the soil profile due to decreased total carbon input into the soil by plants and enhanced decomposition of medium and long term carbon stocks. The different processes governing the carbon cycle for grazed and ungrazed conditions have to be taken into account when drawing any conclusions on the ecosystem-atmosphere exchange from the site at Nam Co.

5 Related Work

Studies on carbon cycling on the central Tibetan Plateau have focused mainly on the *Kobresia* pastures (e.g, Ohtsuka et al., 2008; Babel et al., 2014; Zhang et al., 2016, 2018). The alpine *Kobresia* pastures represent an overall small sink of carbon dioxide, but its strength is highly variable within a year, as well as between several years (Gu et al., 2003; Kato et al., 2004, 2006; Saito et al., 2009). While alpine pastures have been studied extensively, the alpine steppe ecosystem has experienced relatively little interest, although it covers a much larger area. This can be explained by difficult accessibility and corresponding under-representation of (micro-) meteorological measurements. While the principal drivers of ecosystem-atmosphere CO_2 exchange seem to be similar in alpine steppe and pasture ecosystems, Ganjurjav et al. (2016) showed that warming significantly stimulated plant growth in the alpine pastures, but reduced growth and diversity in the alpine steppe ecosystem. Findings for the alpine steppe ecosystem suggest overall high correlation between soil water content and CO_2 fluxes, while it could not be clarified, whether the alpine steppe acts as an overall sink or source of CO_2 (Zhu et al., 2015; Wang et al., 2016). The fluxes varied substantially between the years depending on onset and strength of the monsoonal precipitation and temperature, indicating a close ~~relationship to~~ correlation with the strong seasonality on the TP. Interestingly, the high solar radiation seems to hamper diurnal carbon uptake by exceeding the maximum photosynthetic capacity during noon. Wei et al. (2012) conducted

chamber measurements at Nam Co, corroborating the small sink strength for the growing seasons 2009 and 2010. This study is the first to report long-term, year-round CO_2 fluxes from the alpine steppe ecosystem which may be used to better understand carbon cycling under accelerated climate change scenarios.

6 Conclusions

Here, we present the first long term eddy covariance (EC) CO_2 and H_2O flux measurements from the alpine steppe ecosystem which covers roughly 800,000 km^2 on the central Tibetan Plateau. The harsh environmental conditions and the remote location at > 4500 m above sea level make continuous and high-quality measurements especially challenging. To ensure meaningful flux estimates, we applied rigorous quality filtering rules and analyzed the turbulent flow regime to identify erroneous data. We efficiently removed a drift in mean concentration measurements, possibly caused by dirt contamination in the optical path and ~~aging~~ ageing internal chemicals of the IRGA (Fratini et al., 2014). Furthermore, we ~~corrected the CO_2 flux measurements for~~ found that the sensor self heating ~~effects~~ effect during cold conditions only plays a minor role at our study site. When applying the standard Burba et al. (2008) self heating correction and the revised formulations by Frank and Massman (2020), we clearly see an overcompensation of the SSH effect. High solar radiation and midday soil surface temperatures well above 0 °C suggest that the small carbon uptake during winter daytime may indeed be a physiological meaningful signal rather than an artifact. ~~Following Oechel et al. (2014), we were able to address the site-specific inclination of the open path IRGA rather than using the default corrections factors for vertically aligned sensors (Burba et al., 2008).~~ The wind direction distributions of wind speed and TKE ~~, as well as the analysis of cumulative footprints~~ suggest that the several buildings which were constructed in close vicinity of the tower do exert some influence on the flow regime~~while not violating basic EC assumptions. Nevertheless, fluxes originating mainly~~ . Fluxes originating from the disturbed areas should be excluded from further analyses as they may be compromised by human activities. Data availability of CO_2 fluxes after quality filtering and gap filling is quite different for individual years. While seven complete years of CO_2 ecosystem-atmosphere exchange are available, the filled data gaps are quite large, covering up to two months and should therefore be interpreted carefully. Unfortunately, the whole research station was fenced in 2006, thus preventing the otherwise ubiquitous yak, goat and sheep from grazing within the footprint. While biogeochemical cycles react quite slowly on the grazing exclosure, there is certainly some influence on vegetation and soil properties which should be subject to further examination.

Nearly 15 years of consistently processed and quality controlled CO_2 flux data from the large but underrepresented Tibeten alpine steppe ecosystem are a valuable addition to further deepen the knowledge on carbon cycling in high alpine grassland ecosystems, which are especially vulnerable to global warming. The presented data set covers CO_2 and H_2O fluxes with quality flags for each processing step, footprint modeling and NEE gap filling results, as well as auxiliary measurements of meteorological variables and can be accessed via https://www.doi.org/10.5281/zenodo~~.3733203~~ .3733202 (Nieberding et al., 2020a) and https://www.doi.org/10.11888/Meteoro.tpdc.270333 (Nieberding et al., 2020b). This comprehensive data set allows potential users to put the gas flux dynamics into context with ecosystem properties, potential flux drivers and allows for comparison with other data sets.

7 Code and data availability

The data set was uploaded to Zenodo and is freely available under https://www.doi.org/10.5281/zenodo.3733202 (Nieberding et al., 2020a). Furthermore, the data set is available on the National Tibetan Plateau Center and can be accessed through https://www.doi.org/10.11888/Meteoro.tpdc.270333 (Nieberding et al., 2020b) after user registration on the website. The data sets are published under Creative Commons Attribution 4.0 International (CC BY 4.0) license. The R scripts used in this study are provided in the supplementary material of this manuscript.

Appendix A: Processing of meteorological parameters

The PBL tower in close vicinity to the EC system provides additional measurements of air temperature (Ta), relative humidity (RH), wind speed (WS) and wind direction (WD) in several heights, as well as soil temperature (Ts), soil moisture (SMC) and soil heat flux (SHF) in several depths (see Sect. 2.1). A four component radiometer provides measurements of short and long wave incoming and outgoing radiation (SWin, LWin, SWout, LWout, respectively) and a net radiometer provides global radiation (GR). Furthermore, measurements of air pressure (Pa) are available. As a first step, time periods with obviously incorrect measurements were removed. Secondly, we set upper and lower thresholds for every measurement in order to removed physically implausible values from the time series: 30 °C < Ta < -35 °C; 100 % < RH / SMC < 0 %; 1000 W m^{-2} < SHF < -500 W m^{-2}; 1500 W m^{-2} < GR / SWin / SWout (values < 0 W m^{-2} were set to zero); 410 W m^{-2} < LWin < 75 W m^{-2}; 750 W m^{-2} < LWout < 150 W m^{-2}; 600 hPa < Pa < 500 hPa. ~~The soil temperature in 20 cm depth was additionally despiked using the same method as in Sect. 2.4.~~ In order to produce a time series as complete as possible, we merged biometeorological variables when possible. The low frequency air temperature and relative humidity measurements from the EC tower were filled step wise with the respective measurements from the different heights of the PBL tower, depending on their correlation (2 m > 4 m > 1.5 m > 10 m > 20 m). For Ts, the measurements from 0 cm depth were filled with the measurements from 10 cm and 20 cm depth. For SMC and SHF, the measurements from 10 cm depth were filled with the respective measurements from 20 cm depth. For the short and long wave radiation components, additional measurements for the years 2016 and 2017 were available and used when needed. As a last step, data gaps up to one hour (two time-steps) were linearly interpolated. The resulting time series were used as biometeorological input data for EddyPro and are supplied with the data set.

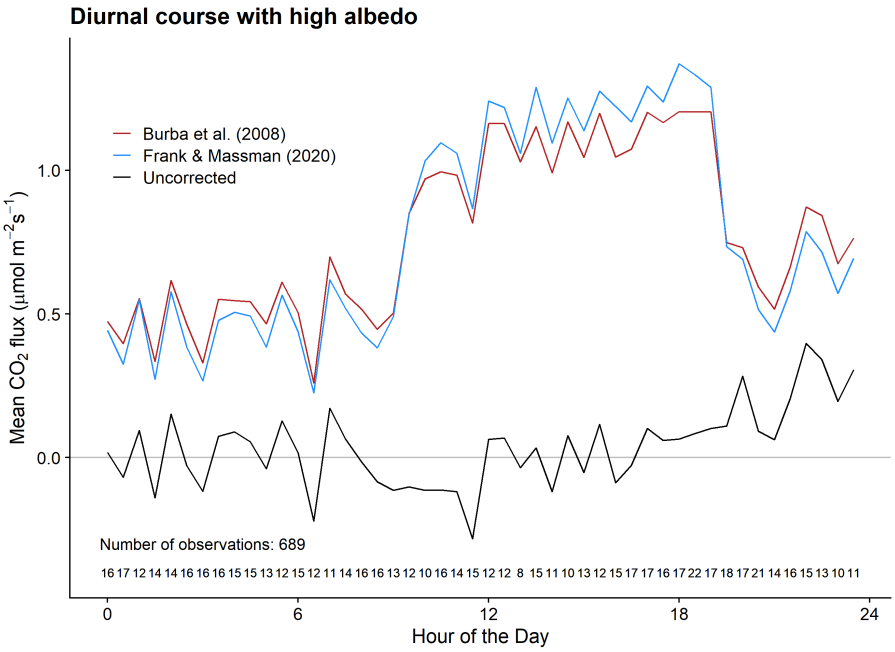

Figure A1. Mean diurnal course of the original and SSH corrected (Burba et al., 2008; Frank and Massman, 2020) CO_2 flux, during cold periods (air temperature < 0 °C) and closed snow cover (short wave albedo > 0.8). Note that a closed snow cover is rarely found at our site, therefore the number of data points is limited. Most data originate from the winter of 2006-2007.

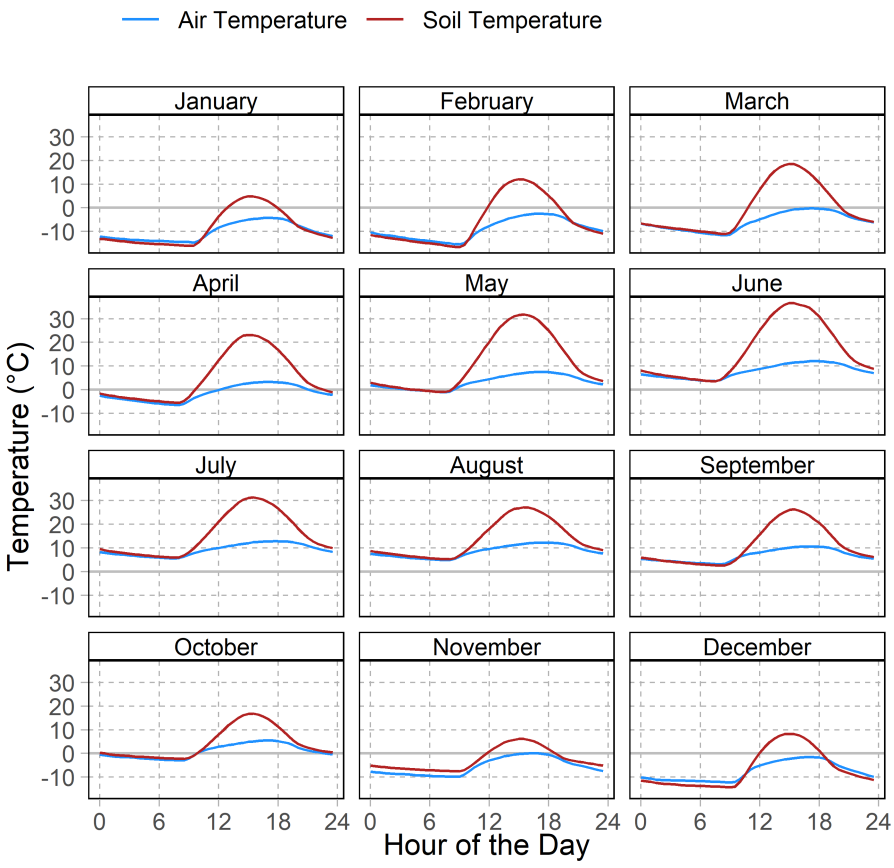

Figure A2. Monthly mean daily course of air and soil temperatures of the years 2005 to 2019.

Table A1. Data availability after individual processing and filtering steps. All units in % of the whole year, respectively

	CO_2 fluxes					H_2O fluxes			
Year	Raw	Wind dir.	Ustar	QC	Gap filling	Raw	Wind dir.	Ustar	QC
2005	7.3	6.1	5.0	4.5	7.4	7.3	5.8	4.7	4.2
2006	55.0	42.8	38.2	33.1	100	55.0	41.1	36.4	31.9
2007	75.6	61.0	55.0	48.0	100	75.5	61.1	55.0	48.2
2008	86.9	69.2	63.4	54.7	100	86.1	67.2	61.7	53.9
2009	92.8	72.0	65.1	57.0	100	92.8	69.7	62.9	56.1
2010	71.4	48.0	41.8	35.6	100	71.4	46.5	40.4	34.8
2011	65.0	41.2	36.6	31.3	100	65.0	41.3	36.8	31.7
2012	19.2	11.7	10.4	9.0	41.3	19.2	11.6	10.3	8.9
2013	0.2	0.0	0.0	0.0	2.7	0.2	0.0	0.0	0.0
2014	26.5	17.8	16.7	14.1	32.9	26.2	17.5	16.4	13.7
2015	40.1	23.7	20.9	18.5	62.2	40.0	23.0	20.2	18.0
2016	48.2	30.5	27.8	23.6	84.9	48.3	30.0	27.4	24.0
2017	77.0	49.7	44.7	37.4	100	77.0	49.1	44.2	37.6
2018	30.5	15.7	13.7	11.8	30.8	30.5	14.8	13.0	11.3
2019	21.4	13.5	12.4	10.2	33.1	21.1	13.2	12.2	9.5

Author contributions. TS, CW and YM conceptualized and administered the research activity planning and execution and acquired funds for it. FN, MOA and YW conducted the investigation. FN, CW, GF and MOA analyzed the data. FN and MOA created the visualizations. FN wrote the original draft. FN, CW, GF, MOA, YW, YM and TS reviewed and edited the original draft.

Competing interests. The authors declare that they have no conflict of interest.

Acknowledgements. We thank George Burba for providing the Excel spreadsheets from which the initial calculations of the sensor self heating correction were derived. Special thanks go to Guoshuai Zhang and Binbin Wang who were a great help during field work and to Guoshuai Zhang for providing the aerial images used in Figs. 1, 2~~and ??~~. We thank Prof. Li Jia from the Institute of Remote Sensing and Digital Earth (CAS) for providing additional radiation data. This research is a contribution to the International Research Training Group "Geo-ecosystems in transition on the Tibetan Plateau (TransTiP)", funded by Deutsche Forschungsgemeinschaft (DFG grant 317513741 / GRK 2309). It was supported by the Second Tibetan Plateau Scientific Expedition and Research (STEP) program (2019QZKK0103), the Strategic Priority Research Program of Chinese Academy of Sciences (XDA20060101) and the National Natural Science Foundation of China (91837208). We acknowledge support by the Open Access Publication Funds of the Technische Universität Braunschweig.

References

Aubinet, M., Vesala, T., and Papale, D.: Eddy Covariance, Springer Netherlands, Dordrecht, 2012.

Babel, W., Biermann, T., Coners, H., Falge, E., Seeber, E., Ingrisch, J., Schleuß, P.-M., Gerken, T., Leonbacher, J., Leipold, T., Willinghöfer, S., Schützenmeister, K., Shibistova, O., Becker, L., Hafner, S., Spielvogel, S., Li, X., Xu, X., Sun, Y., Zhang, L., Yang, Y., Ma, Y., Wesche, K., Graf, H., Leuschner, C., Guggenberger, G., Kuzyakov, Y., Miehe, G., and Foken, T.: Pasture degradation modifies the water and carbon cycles of the Tibetan highlands, Biogeosciences, 11, 6633–6656, https://doi.org/10.5194/bg-11-6633-2014, 2014.

Bate, G. C. and Smith, V. R.: Photosynthesis and respiration in the Sub-Antarctic tussock grass Poa cookii, The New phytologist, 95, 533–543, https://doi.org/10.1111/j.1469-8137.1983.tb03518.x, 1983.

Biermann, T., Babel, W., Ma, W., Chen, X., Thiem, E., Ma, Y., and Foken, T.: Turbulent flux observations and modelling over a shallow lake and a wet grassland in the Nam Co basin, Tibetan Plateau, Theoretical and Applied Climatology, 116, 301–316, https://doi.org/10.1007/s00704-013-0953-6, 2014.

Burba, G. G., McDermitt, D. K., Grelle, A., Anderson, D., and XU, L.: Addressing the influence of instrument surface heat exchange on the measurements of CO 2 flux from open-path gas analyzers, Global Change Biology, 14, 1854–1876, https://doi.org/10.1111/j.1365-2486.2008.01606.x, 2008.

Cuo, L. and Zhang, Y.: Spatial patterns of wet season precipitation vertical gradients on the Tibetan Plateau and the surroundings, Scientific reports, 7, 5057, https://doi.org/10.1038/s41598-017-05345-6, https://doi.org/10.1038/s41598-017-05345-6, 2017.

Dlugokencky, E. J., Mund, J. W., Crotwell, A. M., Crotwell, M. J., and Thoning, K. W.: Atmospheric Carbon Dioxide Dry Air Mole Fractions from the NOAA GML Carbon Cycle Cooperative Global Air Sampling Network, 1968-2019: Version: 2020-07, https://doi.org/10.15138/wkgj-f215, 2020.

El-Madany, T. S., Reichstein, M., Perez-Priego, O., Carrara, A., Moreno, G., Pilar Martín, M., Pacheco-Labrador, J., Wohlfahrt, G., Nieto, H., Weber, U., Kolle, O., Luo, Y.-P., Carvalhais, N., and Migliavacca, M.: Drivers of spatio-temporal variability of carbon dioxide and energy fluxes in a Mediterranean savanna ecosystem, Agricultural and Forest Meteorology, 262, 258–278, https://doi.org/10.1016/j.agrformet.2018.07.010, 2018.

Falge, E., Baldocchi, D., Olson, R., Anthoni, P., Aubinet, M., Bernhofer, C., Burba, G., Ceulemans, R., Clement, R., Dolman, H., Granier, A., Gross, P., Grünwald, T., Hollinger, D., Jensen, N.-O., Katul, G. G., Keronen, P., Kowalski, A., Lai, C. T., Law, B. E., Meyers, T., Moncrieff, J., Moors, E., Munger, W., Pilegaard, K., Rannik, Ü., Rebmann, C., Suyker, A., Tenhunen, J., Tu, K., Verma, S., Vesala, T., Wilson, K., and Wofsy, S.: Gap filling strategies for defensible annual sums of net ecosystem exchange, Agricultural and Forest Meteorology, 107, 43–69, https://doi.org/10.1016/S0168-1923(00)00225-2, 2001.

Finkelstein, P. L. and Sims, P. F.: Sampling error in eddy correlation flux measurements, Journal of Geophysical Research: Atmospheres, 106, 3503–3509, https://doi.org/10.1029/2000JD900731, 2001.

Foken, T. and Wichura, B.: Tools for quality assessment of surface-based flux measurements, Agricultural and Forest Meteorology, 78, 83–105, https://doi.org/10.1016/0168-1923(95)02248-1, 1996.

Foken, T., Göckede, M., Mauder, M., Mahrt, L., Amiro, B., and Munger, W.: Post-Field Data Quality Control, in: Handbook of micrometeorology, edited by Lee, X., Massman, W. J., and Law, B. E., vol. 29 of *Atmospheric and Oceanographic Sciences Library*, pp. 181–208, Kluwer Academic Publishers, Dordrecht and Boston and London, 2004.

Frank, J. M. and Massman, W. J.: A new perspective on the open-path infrared gas analyzer self-heating correction, Agricultural and Forest Meteorology, 290, 107 986, https://doi.org/10.1016/j.agrformet.2020.107986, 2020.

Fratini, G., McDermitt, D. K., and Papale, D.: Eddy-covariance flux errors due to biases in gas concentration measurements: origins, quantification and correction, Biogeosciences, 11, 1037–1051, https://doi.org/10.5194/bg-11-1037-2014, 2014.

Ganjurjav, H., Gao, Q., Gornish, E. S., Schwartz, M. W., Liang, Y., Cao, X., Zhang, W., Zhang, Y., Li, W., Wan, Y., Li, Y., Danjiu, L., Guo, H., and Lin, E.: Differential response of alpine steppe and alpine meadow to climate warming in the central Qinghai–Tibetan Plateau, Agricultural and Forest Meteorology, 223, 233–240, https://doi.org/10.1016/j.agrformet.2016.03.017, 2016.

Gu, S., Tang, Y., Du, M., Kato, T., Li, Y., Cui, X., and Zhao, X.: Short-term variation of CO2 flux in relation to environmental controls in an alpine meadow on the Qinghai-Tibetan Plateau, Journal of Geophysical Research: Atmospheres, 108, 711, https://doi.org/10.1029/2003JD003584, 2003.

Hafner, S., Unteregelsbacher, S., Seeber, E., Lena, B., Xu, X., Li, X., Guggenberger, G., Miehe, G., and Kuzyakov, Y.: Effect of grazing on carbon stocks and assimilate partitioning in a Tibetan montane pasture revealed by 13CO2 pulse labeling, Global Change Biology, 18, 528–538, https://doi.org/10.1111/j.1365-2486.2011.02557.x, 2012.

Holl, D., Wille, C., Sachs, T., Schreiber, P., Runkle, B. R. K., Beckebanze, L., Langer, M., Boike, J., Pfeiffer, E.-M., Fedorova, I., Bolshianov, D. Y., Grigoriev, M. N., and Kutzbach, L.: A long-term (2002 to 2017) record of closed-path and open-path eddy covariance CO₂ net ecosystem exchange fluxes from the Siberian Arctic, Earth System Science Data, 11, 221–240, https://doi.org/10.5194/essd-11-221-2019, 2019.

Kappen, L., Schroeter, B., Scheidegger, C., Sommerkorn, M., and Hestmark, G.: Cold resistance and metabolic activity of lichens below 0°C, Advances in Space Research, 18, 119–128, https://doi.org/10.1016/0273-1177(96)00007-5, 1996.

Kato, T., Tang, Y., Song, G., Hirota, M., Cui, X., Du, M., Li, Y., Zhao, X., and Oikawa, T.: Seasonal patterns of gross primary production and ecosystem respiration in an alpine meadow ecosystem on the Qinghai-Tibetan Plateau, Journal of Geophysical Research, 109, 711, https://doi.org/10.1029/2003JD003951, 2004.

Kato, T., Tang, Y., Gu, S., Hirota, M., Du, M., Li, Y., and Zhao, X.: Temperature and biomass influences on interannual changes in CO2 exchange in an alpine meadow on the Qinghai-Tibetan Plateau, Global Change Biology, 12, 1285–1298, https://doi.org/10.1111/j.1365-2486.2006.01153.x, 2006.

Kormann, R. and Meixner, F. X.: An Analytical Footprint Model For Non-Neutral Stratification, Boundary-Layer Meteorology, 99, 207–224, https://doi.org/10.1023/A:1018991015119, 2001.

Li, J., Yan, D., Pendall, E., Pei, J., Noh, N. J., He, J.-S., Li, B., Nie, M., and Fang, C.: Depth dependence of soil carbon temperature sensitivity across Tibetan permafrost regions, Soil Biology and Biochemistry, 126, 82–90, 2018.

Liu, H., Randerson, J. T., Lindfors, J., Massman, W. J., and Foken, T.: Consequences of Incomplete Surface Energy Balance Closure for CO2 Fluxes from Open-Path CO2/H2O Infrared Gas Analysers, Boundary-Layer Meteorology, 120, 65–85, https://doi.org/10.1007/s10546-005-9047-z, https://doi.org/10.1007/s10546-005-9047-z, 2006.

Ma, Y., Wang, Y., Wu, R., Hu, Z., Yang, K., Li, M., Ma, W., Zhong, L., Sun, F., Chen, X., Zhu, Z., Wang, S., and Ishikawa, H.: Recent advances on the study of atmosphere-land interaction observations on the Tibetan Plateau, Hydrology and Earth System Sciences, 13, 1103–1111, https://doi.org/10.5194/hess-13-1103-2009, 2009.

Mauder, M. and Foken, T.: Impact of post-field data processing on eddy covariance flux estimates and energy balance closure, Meteorologische Zeitschrift, 15, 597–609, https://doi.org/10.1127/0941-2948/2006/0167, 2006.

Mauder, M., Cuntz, M., Drüe, C., Graf, A., Rebmann, C., Schmid, H. P., Schmidt, M., and Steinbrecher, R.: A strategy for quality and uncertainty assessment of long-term eddy-covariance measurements, Agricultural and Forest Meteorology, 169, 122–135, https://doi.org/10.1016/j.agrformet.2012.09.006, 2013.

Miehe, G., Bach, K., Miehe, S., Kluge, J., Yongping, Y., La Duo, Co, S., and Wesche, K.: Alpine steppe plant communities of the Tibetan highlands, Applied Vegetation Science, 14, 547–560, https://doi.org/10.1111/j.1654-109X.2011.01147.x, 2011.

Miehe, G., Schleuss, P.-M., Seeber, E., Babel, W., Biermann, T., Braendle, M., Chen, F., Coners, H., Foken, T., Gerken, T., Graf, H.-F., Guggenberger, G., Hafner, S., Holzapfel, M., Ingrisch, J., Kuzyakov, Y., Lai, Z., Lehnert, L., Leuschner, C., Li, X., Liu, J., Liu, S., Ma, Y., Miehe, S., Mosbrugger, V., Noltie, H. J., Schmidt, J., Spielvogel, S., Unteregelsbacher, S., Wang, Y., Willinghöfer, S., Xu, X., Yang, Y., Zhang, S., Opgenoorth, L., and Wesche, K.: The Kobresia pygmaea ecosystem of the Tibetan highlands - Origin, functioning and degradation of the world's largest pastoral alpine ecosystem: Kobresia pastures of Tibet, The Science of the total environment, 648, 754–771, https://doi.org/10.1016/j.scitotenv.2018.08.164, 2019.

Moncrieff, J., Clement, R., Finnigan, J., and Meyers, T.: Averaging, Detrending, and Filtering of Eddy Covariance Time Series, in: Handbook of Micrometeorology: A Guide for Surface Flux Measurement and Analysis, edited by Lee, X., Massman, W., and Law, B., pp. 7–31, Springer Netherlands, Dordrecht, https://doi.org/10.1007/1-4020-2265-4_2, 2005.

Moncrieff, J. B., Massheder, J. M., de Bruin, H., Elbers, J., Friborg, T., Heusinkveld, B., Kabat, P., Scott, S., Soegaard, H., and Verhoef, A.: A system to measure surface fluxes of momentum, sensible heat, water vapour and carbon dioxide, Journal of Hydrology, 188-189, 589–611, https://doi.org/10.1016/S0022-1694(96)03194-0, 1997.

NASA/METI/AIST/Japan Spacesystems, and U.S./Japan ASTER Science Team: ASTER Global Digital Elevation Model V003, distributed by NASA EOSDIS Land Processes DAAC, https://doi.org/10.5067/ASTER/ASTGTM.003, 2019.

Nieberding, F., Ma, Y., Wille, C., Fratini, G., Asmussen, M. O., Wang, Y., Ma, W., and Sachs, T.: A long term hourly eddy covariance dataset of consistently processed CO2 and H2O Fluxes from the Tibetan Alpine Steppe at Nam Co (2005 - 2019) [Data set]., Zenodo, https://doi.org/10.5281/ZENODO.3733202, 2020a.

Nieberding, F., Ma, Y., Wille, C., Fratini, G., Asmussen, M. O., Wang, Y., Ma, W., and Sachs, T.: A long term hourly eddy covariance dataset of consistently processed CO2 and H2O Fluxes from the Tibetan Alpine Steppe at Nam Co (2005 - 2019), National Tibetan Plateau Data Center, https://doi.org/10.11888/Meteoro.tpdc.270333, 2020b.

NOAA ESRL Global Monitoring Division: Atmospheric Carbon Dioxide Dry Air Mole Fractions from quasi-continuous measurements at Mauna Loa, Hawaii, Barrow, Alaska, American Samoa and South Pole. Compiled by K.W. Thoning, D.R. Kitzis, and A. Crotwell., https://doi.org/10.15138/yaf1-bk21.

Nölling, J.: Satellitenbildgestützte Vegetationskartierung von Hochweidegebieten des Tibetischen Plateaus auf Grundlage von plotbasierten Vegetationsaufnahmen mit multivariater statistischer Analyse: Ein Beitrag zum Umweltmonitoring, Diplomarbeit, Universität Marburg, Marburg, 2006.

Oechel, W. C., Laskowski, C. A., Burba, G., Gioli, B., and Kalhori, A. A. M.: Annual patterns and budget of CO 2 flux in an Arctic tussock tundra ecosystem, Journal of Geophysical Research: Biogeosciences, 119, 323–339, https://doi.org/10.1002/2013JG002431, 2014.

Ohtsuka, T., Hirota, M., Zhang, X., Shimono, A., Senga, Y., Du, M., Yonemura, S., Kawashima, S., and Tang, Y.: Soil organic carbon pools in alpine to nival zones along an altitudinal gradient (4400–5300m) on the Tibetan Plateau, Polar Science, 2, 277–285, https://doi.org/10.1016/j.polar.2008.08.003, 2008.

Panikov, N. S., Flanagan, P. W., Oechel, W. C., Mastepanov, M. A., and Christensen, T. R.: Microbial activity in soils frozen to below −39°C, Soil Biology and Biochemistry, 38, 785–794, https://doi.org/10.1016/j.soilbio.2005.07.004, 2006.

Papale, D., Reichstein, M., Aubinet, M., Canfora, E., Bernhofer, C., Kutsch, W., Longdoz, B., Rambal, S., Valentini, R., Vesala, T., and Yakir, D.: Towards a standardized processing of Net Ecosystem Exchange measured with eddy covariance technique: algorithms and uncertainty estimation, Biogeosciences, 3, 571–583, https://doi.org/10.5194/bg-3-571-2006, 2006.

Qiu, J.: China: The third pole, Nature, 454, 393–396, https://doi.org/10.1038/454393a, 2008.

Reichstein, M., Falge, E., Baldocchi, D., Papale, D., Aubinet, M., Berbigier, P., Bernhofer, C., Buchmann, N., Gilmanov, T., Granier, A., Grunwald, T., Havrankova, K., Ilvesniemi, H., Janous, D., Knohl, A., Laurila, T., Lohila, A., Loustau, D., Matteucci, G., Meyers, T., miglietta, F., ourcival, J.-m., Pumpanen, J., Rambal, S., Rotenberg, E., Sanz, M., Tenhunen, J., Seufert, G., Vaccari, F., Vesala, T., Yakir, D., and valentini, R.: On the separation of net ecosystem exchange into assimilation and ecosystem respiration: review and improved algorithm, Global Change Biology, 11, 1424–1439, https://doi.org/10.1111/j.1365-2486.2005.001002.x, 2005.

Richardson, A. D., Aubinet, M., Barr, A. G., Hollinger, D. Y., Ibrom, A., Lasslop, G., and Reichstein, M.: Uncertainty Quantification, in: Eddy Covariance: A Practical Guide to Measurement and Data Analysis, edited by Aubinet, M., Vesala, T., and Papale, D., pp. 173–209, Springer Netherlands, Dordrecht, https://doi.org/10.1007/978-94-007-2351-1_7, https://doi.org/10.1007/978-94-007-2351-1_7, 2012.

Saito, M., Kato, T., and Tang, Y.: Temperature controls ecosystem CO 2 exchange of an alpine meadow on the northeastern Tibetan Plateau, Global Change Biology, 15, 221–228, https://doi.org/10.1111/j.1365-2486.2008.01713.x, 2009.

Serrano-Ortiz, P., Kowalski, A. S., Domingo, F., Ruiz, B., and Alados-Arboledas, L.: Consequences of Uncertainties in CO2 Density for Estimating Net Ecosystem CO2 Exchange by Open-path Eddy Covariance, Boundary-Layer Meteorology, 126, 209–218, https://doi.org/10.1007/s10546-007-9234-1, 2008.

Vaisala: Vaisala HUMICAP® Humidity and Temperature Probes HMP45A/D: HMP45A and HMP45D Operating Manual, https://www.vaisala.com/sites/default/files/documents/HMP45AD-User-Guide-U274EN.pdf, 2006.

Vickers, D. and Mahrt, L.: Quality Control and Flux Sampling Problems for Tower and Aircraft Data, Journal of Atmospheric and Oceanic Technology, 14, 512–526, https://doi.org/10.1175/1520-0426(1997)014<0512:QCAFSP>2.0.CO;2, 1997.

Wang, L., Liu, H., Shao, Y., Liu, Y., and Sun, J.: Water and CO2 fluxes over semiarid alpine steppe and humid alpine meadow ecosystems on the Tibetan Plateau, Theoretical and Applied Climatology, 131, 547–556, https://doi.org/10.1007/s00704-016-1997-1, 2016.

Wang, X., Pang, G., and Yang, M.: Precipitation over the Tibetan Plateau during recent decades: a review based on observations and simulations, International Journal of Climatology, 38, 1116–1131, https://doi.org/10.1002/joc.5246, 2018.

Webb, E. K., Pearman, G. I., and Leuning, R.: Correction of flux measurements for density effects due to heat and water vapour transfer, Quarterly Journal of the Royal Meteorological Society, 106, 85–100, 1980.

Wei, D., Ri, X., Wang, Y., Wang, Y., Liu, Y., and Yao, T.: Responses of CO2, CH4 and N2O fluxes to livestock exclosure in an alpine steppe on the Tibetan Plateau, China, Plant and Soil, 359, 45–55, https://doi.org/10.1007/s11104-011-1105-3, 2012.

Wutzler, T., Lucas-Moffat, A., Migliavacca, M., Knauer, J., Sickel, K., Šigut, L., Menzer, O., and Reichstein, M.: Basic and extensible post-processing of eddy covariance flux data with REddyProc, Biogeosciences, 15, 5015–5030, https://doi.org/10.5194/bg-15-5015-2018, 2018.

Yang, K., Wu, H., Qin, J., Lin, C., Tang, W., and Chen, Y.: Recent climate changes over the Tibetan Plateau and their impacts on energy and water cycle: A review, Global and Planetary Change, 112, 79–91, https://doi.org/10.1016/j.gloplacha.2013.12.001, 2014.

Yao, T., Xue, Y., Chen, D., Chen, F., Thompson, L., Cui, P., Koike, T., Lau, W. K.-M., Lettenmaier, D., Mosbrugger, V., Zhang, R., Xu, B., Dozier, J., Gillespie, T., Gu, Y., Kang, S., Piao, S., Sugimoto, S., Ueno, K., Wang, L., Wang, W., Zhang, F., Sheng, Y., Guo, W., Ailikun, Yang, X., Ma, Y., Shen, S. S. P., Su, Z., Chen, F., Liang, S., Liu, Y., Singh, V. P., Yang, K., Yang, D., Zhao, X., Qian, Y., Zhang, Y., and Li, Q.: Recent Third Pole's Rapid Warming Accompanies Cryospheric Melt and Water Cycle Intensification and Interactions between Monsoon and Environment: Multidisciplinary Approach with Observations, Modeling, and Analysis, Bulletin of the American Meteorological Society, 100, 423–444, https://doi.org/10.1175/BAMS-D-17-0057.1, 2019.

Zhang, T., Zhang, Y., Xu, M., Xi, Y., Zhu, J., Zhang, X., Wang, Y., Li, Y., Shi, P., Yu, G., and Sun, X.: Ecosystem response more than climate variability drives the inter-annual variability of carbon fluxes in three Chinese grasslands, Agricultural and Forest Meteorology, 225, 48–56, https://doi.org/10.1016/j.agrformet.2016.05.004, 2016.

Zhang, T., Zhang, Y., Xu, M., Zhu, J., Chen, N., Jiang, Y., Huang, K., Zu, J., Liu, Y., and Yu, G.: Water availability is more important than temperature in driving the carbon fluxes of an alpine meadow on the Tibetan Plateau, Agricultural and Forest Meteorology, 256-257, 22–31, https://doi.org/10.1016/j.agrformet.2018.02.027, 2018.

Zhou, Y., Webster, R., Viscarra Rossel, R. A., Shi, Z., and Chen, S.: Baseline map of soil organic carbon in Tibet and its uncertainty in the 1980s, Geoderma, 334, 124–133, https://doi.org/10.1016/j.geoderma.2018.07.037, 2019.

Zhu, Z., Ma, Y., Li, M., Hu, Z., Xu, C., Zhang, L., Han, C., Wang, Y., and Ichiro, T.: Carbon dioxide exchange between an alpine steppe ecosystem and the atmosphere on the Nam Co area of the Tibetan Plateau, Agricultural and Forest Meteorology, 203, 169–179, https://doi.org/10.1016/j.agrformet.2014.12.013, 2015.